Science of the Total Environment 630 (2018) 630–647

Contents lists available at ScienceDirect

Science of the Total Environment

journal homepage: www.elsevier.com/locate/scitotenv

Terrestrial dissolved organic matter distribution in the North Sea

Stuart C. Painter [a,*], Dan J. Lapworth [b], E. Malcolm S. Woodward [c], Silke Kroeger [d], Chris D. Evans [e], Daniel J. Mayor [a], Richard J. Sanders [a]

[a] National Oceanography Centre, Southampton, UK
[b] British Geological Survey, Wallingford, UK
[c] Plymouth Marine Laboratory, Plymouth, UK
[d] Centre for Environment, Fisheries and Aquaculture Science, Lowestoft, UK
[e] Centre for Ecology and Hydrology, Environment Centre Wales, Bangor, UK

HIGHLIGHTS

- North Sea fluorescent DOM field sampled to map terrestrial inputs and distributions.
- DOM pool characterised via absorbance and excitation-emission fluorescent spectra.
- Three distinct FDOM fluorophores identified.
- No clear evidence found for significant terrestrial DOM export to the Atlantic Ocean.
- North Sea terrestrial DOM distributions appear stable over multi-decadal timescales.

GRAPHICAL ABSTRACT

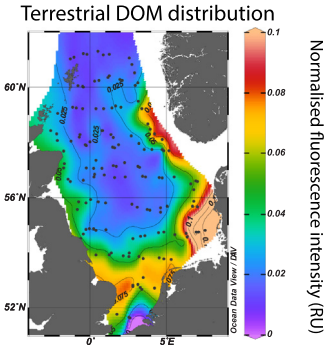

ARTICLE INFO

Article history:
Received 22 December 2017
Received in revised form 19 February 2018
Accepted 19 February 2018
Available online xxxx

Editor: Jay Gan

Keywords:
Absorption
Fluorescent dissolved organic matter (FDOM)
Chromophoric dissolved organic matter (CDOM)
Dissolved organic carbon (DOC)
Excitation-Emission Matrix Parallel Factor analysis (EEM-PARAFAC)
North Sea
Biogeochemistry

ABSTRACT

The flow of terrestrial carbon to rivers and inland waters is a major term in the global carbon cycle. The organic fraction of this flux may be buried, remineralized or ultimately stored in the deep ocean. The latter can only occur if terrestrial organic carbon can pass through the coastal and estuarine filter, a process of unknown efficiency. Here, data are presented on the spatial distribution of terrestrial fluorescent and chromophoric dissolved organic matter (FDOM and CDOM, respectively) throughout the North Sea, which receives organic matter from multiple distinct sources. We use FDOM and CDOM as proxies for terrestrial dissolved organic matter (tDOM) to test the hypothesis that tDOM is quantitatively transferred through the North Sea to the open North Atlantic Ocean. Excitation emission matrix fluorescence and parallel factor analysis (EEM-PARAFAC) revealed a single terrestrial humic-like class of compounds whose distribution was restricted to the coastal margins and, via an inverse salinity relationship, to major riverine inputs. Two distinct sources of fluorescent humic-like material were observed associated with the combined outflows of the Rhine, Weser and Elbe rivers in the south-eastern North Sea and the Baltic Sea outflow to the eastern central North Sea. The flux of tDOM from the North Sea to the Atlantic Ocean appears insignificant, although tDOM export may occur through Norwegian coastal waters unsampled in our study. Our analysis suggests that the bulk of tDOM exported from the Northwest European and Scandinavian landmasses is buried or remineralized internally, with potential losses to the atmosphere. This interpretation implies that the residence time in estuarine and coastal systems exerts an important control over the fate of tDOM and needs to be considered when evaluating the role of terrestrial carbon losses in the global carbon cycle.

* Corresponding author at: National Oceanography Centre, European Way, Southampton SO14 3ZH, UK.
E-mail address: stuart.painter@noc.ac.uk (S.C. Painter).

https://doi.org/10.1016/j.scitotenv.2018.02.237

1. Introduction

The flow of terrestrial organic matter (tOM) through aquatic ecosystems is a significant and increasing component of the global carbon cycle (Ciais et al., 2013) and appears to be increasing in some regions, notably Northern Europe (Monteith et al., 2007). Spatial variations in tOM flux are controlled by regional climate, soil type, vegetation and land use, with the fraction of tOM that ultimately reaches the coastal ocean dependent upon additional biotic and abiotic production and removal processes along the land-sea continuum (Yamashita et al., 2011a; Graeber et al., 2012; Ward et al., 2017). However, the relative importance and future evolution of these processes remain poorly understood with key processes relevant to the transport and transformation of tOM missing from Earth System models, despite its recognised importance (Ciais et al., 2013).

Presently, a total global carbon (C) flux from the land to the ocean of approximately 0.9 Pg C occurs annually consisting of ~0.2 Pg as dissolved organic carbon (DOC), 0.3 Pg as dissolved inorganic carbon (DIC) and up to 0.4 Pg as particulate organic carbon (POC) (Bianchi, 2011; Dai et al., 2012; Ciais et al., 2013). The magnitude of this total terrestrial carbon flux is equivalent to approximately one-third of the total annual oceanic CO_2 drawdown (~2.6 Pg C yr^{-1}; Le Quere et al., 2016). Yet despite the terrestrial DOC flux being capable of turning over the entire marine DOC pool of ~700 Pg C on millennial timescales (Hansell et al., 2009), there is only limited evidence for a significant terrestrial contribution to the open ocean DOC pool which suggests rapid removal of tOM inputs in coastal and shelf waters (Hedges et al., 1997; Opsahl and Benner, 1997; Bianchi, 2011).

Most tOM derives from plant exudation, the decomposition of recent litter or soil organic matter (SOM), although some may derive from the breakdown of older SOM, particularly in disturbed soils (Evans et al., 2014; Butman et al., 2015). A significant fraction of this tOM is removed or recycled within inland waterways (Tranvik et al., 2009) but a substantial proportion reaches estuaries and near coastal waters, where it may be subject to further chemical or biological modification, aiding rapid biological utilization and eventual loss to the atmosphere (Bianchi, 2011). The total terrestrial carbon flux of ~0.9 Pg C yr^{-1} that reaches the coastal ocean, is therefore significantly less than the total carbon flux actually lost from terrestrial soils. Estimates vary widely for the various carbon pools, but for the UK it has been estimated that >70% of soil derived DOC entering inland waterways is respired or otherwise lost before it reaches coastal waters (Worrall et al., 2012), which is similar to a global estimate of total organic carbon removal in inland waters obtained by Tranvik et al. (2009). Globally, it is thought that around 25% of soil derived DOC is removed in estuaries alone (Dai et al., 2012). Thus, the global land to ocean DOC flux of ~0.2 Pg C yr^{-1} is acutely sensitive to changes in biotic and abiotic processes which could have significant implications for the proportion of tOM reaching coastal waters. The fate of river borne POC is similar with 30–50% of terrestrially derived POC buried within deltaic sedimentary systems and the remainder rapidly respired in coastal waters (Hedges and Keil, 1995; Burdige, 2005). At present a significant fraction of tOM is prevented from entering the ocean due to processes occurring in freshwater and estuarine systems.

Here we report a North Sea wide survey of chromophoric and fluorescent dissolved organic matter (CDOM and FDOM, respectively) absorbance and fluorescence properties conducted to 1) investigate the mean distribution of terrestrial dissolved organic matter (tDOM) during summer 2016, 2) identify the major tDOM sources, and 3) determine the likely fate of tDOM entering the North Sea. Collectively, CDOM and FDOM represent 20–70% of the overall DOM pool (e.g. Dittmar and Stubbins, 2014), and as tracers of the tDOM pool can underestimate export fluxes, but CDOM and FDOM distributions are nevertheless considered valuable proxies for tDOM more generally (e.g. Stedmon and Nelson, 2015).

2. Methods

2.1. Regional setting

The North Sea is a semi-enclosed marginal sea of the temperate latitude Northeast Atlantic, and part of the larger northwest European continental shelf (Otto et al., 1990). Oceanic water enters the North Sea via the English Channel to the southwest (~51°N), and directly from the North Atlantic Ocean along its northern boundary (~60°N), with the major outflow occurring via the Norwegian Trench to the northeast (Huthnance et al., 2009). Residence times vary from <100 days for water in the Norwegian Trench to ~4 years for water entering the northwest North Sea (Prandle, 1984; Blaas et al., 2001). Brackish water inputs from the Baltic Sea, via the Kattegat, occur along the eastern edge of the North Sea (Gustafsson and Andersson, 2001). Several major European rivers discharge into the southern North Sea including the rivers Rhine, Meuse, Elbe, Weser and Scheldt and all have been associated with significant tDOM input (Warnock et al., 1999; Astoreca et al., 2009).

2.2. Sampling

Sampling was conducted opportunistically during August–September 2016 onboard the *R.V. CEFAS Endeavour*. Near-surface (~5 m depth) seawater was sampled every 2–3 h during the day and analysed for dissolved inorganic and organic nutrients, salinity, chlorophyll-a concentrations, seawater absorbance, and fluorescent organic matter excitation emission spectra.

2.3. Inorganic and organic nutrient concentrations

Inorganic nutrient samples were syringe filtered through 0.22 μm polyethersulfone filters into acid cleaned and "aged" 60 ml HDPE bottles and frozen at −20 °C for subsequent shore-based analysis. Samples were analysed by colorimetry using a Bran and Luebbe 5-channel AAIII segmented flow autoanalyser using standard analytical techniques (Woodward and Rees, 2001). Detection limits were 0.02, 0.01, 0.01 and 0.02 μmol L^{-1} for total nitrate ($NO_3^- + NO_2^-$), NO_2^-, $Si(OH)_4$ and PO_4^{3-} respectively. For calculation of mean concentrations, where some measurements were below the detection limit, the detection limit was used in statistical calculations.

Duplicate organic nutrient samples were syringe filtered through 0.22 μm polyethersulfone filters into 125 ml HDPE bottles and frozen at −20 °C for later analysis. DOC concentrations were measured on a Skalar Formacs total organic carbon analyser. Samples were acidified with 3 M HCl and sparged with O_2 to remove dissolved inorganic carbon prior to analysis. Total dissolved nitrogen (TDN) and total dissolved phosphorous (TDP) were measured following UV oxidation of samples as described by Torres-Valdes et al. (2016). Briefly, after defrosting the samples duplicate 10 ml aliquots of seawater were UV-oxidised for 2 h using two Metrohm 705 UV oxidation units. After oxidation, TDN and TDP were measured as total nitrate and phosphate using a SEAL Analytical QuAAtro autoanalyser and standard GO-SHIP protocols (Hydes et al., 2010). A third un-oxidised aliquot of each seawater sample was separately measured for the dissolved inorganic nutrient content ($NO_3^- + NO_2^-$ and PO_4^{3-}). Dissolved organic nitrogen (DON) and dissolved organic phosphorous (DOP) concentrations were subsequently calculated by difference between the total dissolved and inorganic nutrient concentrations (i.e. $DON = TDN - (NO_3^- + NO_2^-)$). Nutrient reference materials (KANSO, Japan) were analysed regularly to check precision and accuracy (within 1–2%). Analytical detection limits based on measurement standards were 0.02 and 0.01 μmol L^{-1} for total nitrate ($NO_3^- + NO_2^-$) and PO_4^{3-} respectively. Analytical uncertainty associated with DON and DOP measurements was estimated as the root-sum-square of total nutrient uncertainty based on replicate sample analysis and inorganic nutrient uncertainty based on the global uncertainty associated

with the analysis of all calibration standards. The average measurement uncertainties were 0.14 ± 0.11 μmol L^{-1} for DON and 0.011 ± 0.010 μmol L^{-1} for DOP.

2.4. Salinity and chlorophyll concentrations

Salinity samples were collected in glass bottles, capped with a plastic insert and returned to shore for analysis on an Autosal salinometer (model 8400B) calibrated against OSIL standard seawater (P-series). Herein we report salinity as absolute salinity (S_A) using the Thermodynamic Equation of State 2010 (TEOS-10; UNESCO, 2010).

Chlorophyll-*a* concentrations were measured fluorometrically after filtration of 250 ml seawater through 25 mm GF/F filters (~0.7 μm). After filtration, each filter was placed in a 20 ml glass vial, inoculated with 6 ml of 90% acetone and refrigerated in the dark at 4 °C for 18–20 h. Pigment extracts were measured on a Turner Designs "Trilogy" fluorometer calibrated against a pure chlorophyll-a standard (Sigma, UK).

2.5. Optical and fluorescent properties

Spectral absorbance (200–800 nm) was measured on 0.22 μm filtered seawater samples using a Cary 60 UV–Vis spectrometer, a 1 cm quartz cuvette, and Milli-Q water as a baseline reference. Absorption coefficients (units m^{-1}) were obtained from absorbance (unitless) via Eq. (1),

$$a(\lambda) = \frac{2.303\,A(\lambda)}{l} \tag{1}$$

where A is the measured absorbance at wavelength λ, *l* the cuvette length (in meters) and *a* the resulting absorption coefficient.

The CDOM absorption spectrum slope coefficient (S) was modeled in R (R Core Team, 2016) over the wavelength range 300–600 nm using Eq. (2) and the package CDOM (version 0.1; Massicotte and Markager, 2016)

$$a(\lambda) = a(\lambda_0)e^{-S(\lambda_0-\lambda)} + K \tag{2}$$

where λ_0 is a reference wavelength (400 nm) and K is a background constant. The terms a_{375}, S and K were estimated simultaneously via the modeling process. A wavelength of 375 nm was chosen for consistency with previous studies (e.g. Kowalczuk et al., 2006).

The slope ratio (S_R; Helms et al., 2008), which is the ratio of the slope coefficient calculated for UVB (275–295 nm) and UVA (350–400 nm) wavelengths, was calculated using Eq. (3). This was also obtained via the R CDOM package (Massicotte and Markager, 2016).

$$s_R = \frac{S_{275-295}}{S_{350-400}} \tag{3}$$

Spectral fluorescence was measured on 0.22 μm filtered samples using a Cary Eclipse fluorescence spectrophometer with a 1 cm pathlength. Excitation wavelengths ranged from 200 to 400 nm in 5 nm increments with emission spectra measured over 280–500 nm in 2 nm increments. Absorbance based inner filter corrections (Mcknight et al., 2001; Kothawala et al., 2013), and blank (Milli-Q water) subtractions, were applied to all samples before normalization to Raman units (Murphy et al., 2010). The collated sample excitation emission matrices (EEM) were characterised via parallel factor (PARAFAC) analysis (Bro, 1997; Stedmon et al., 2003; Stedmon and Bro, 2008). Excitation wavelengths <240 nm were discarded during PARAFAC modeling due to increased noise at those wavelengths. Analysis was carried out using the drEEM toolbox for MATLAB with non-negativity constraints on all modes and split-half analysis to validate model components (Murphy et al., 2013). A total of 148 EEMs were included in the analysis.

Specific UV absorbance ($SUVA_{254}$; Weishaar et al., 2003) was calculated to provide information on the aromaticity and molecular weight of the bulk DOC pool. Following recent guidance (Murphy et al., 2010; Stedmon and Nelson, 2015) $SUVA_{254}$ was calculated as

$$SUVA_{254} = \frac{\left(\frac{A}{l}\right)}{DOC} \tag{4}$$

where A is the measured absorbance at 254 nm, *l* the cuvette length (in meters) and DOC is the measured DOC concentration in units of mg L^{-1}. $SUVA_{254}$ is reported with units of $m^2\ g^{-1}C$.

3. Results

3.1. Temperature and salinity

Sea surface temperature (conservative temperature; Θ, °C) ranged over 7 °C from a minimum of 12 °C in the Fair Isle Channel (~60°N) to a maximum of 19.2 °C in the extreme southern North Sea (~51.8°N; Fig. 1a). A strong southeast to northwest temperature gradient that followed the bathymetric slope was evident, with warmer waters in the shallow southern and southeastern North Sea (>16 °C) and cooler waters in the deeper north and northwest (<16 °C) areas.

Absolute Salinity (S_A) did not exhibit comparable spatial patterns but instead revealed a complex distribution of lower salinity inputs to the eastern and southeastern North Sea from the Baltic Sea outflow and discharges from the Rhine, Weser and Elbe rivers respectively, and higher salinity inputs to the northern and central North Sea from the North Atlantic Ocean (Fig. 1b). Absolute salinity ranged from 32.34 to 35.41 g kg^{-1} with lowest salinities around the periphery of the North Sea and higher salinities towards the centre.

3.2. Chlorophyll

Surface chlorophyll concentrations ranged from 0.14–6.79 μg L^{-1} but were generally <3 μg L^{-1} (cruise average 1.04 ± 0.95 μg L^{-1}). Highest chlorophyll concentrations (>2 μg L^{-1}) were distributed around the edge of the North Sea with lowest concentrations (<0.5 μg L^{-1}) towards the central North Sea giving the appearance of a gyre-like distribution (Fig. 1c).

3.3. Inorganic nutrients

Inorganic nutrient concentrations were generally low in the surface waters of the North Sea (Table 1). Total dissolved oxidised nitrogen (also called total nitrate, $NO_3^- + NO_2^-$) ranged from <0.02 to 4.98 (mean 0.31 ± 0.63) μmol L^{-1} with two dominant signatures associated with the Rhine-Meuse-Scheldt delta and waters around the Orkney Islands, where concentrations exceeded 1.5 μmol L^{-1} (Fig. 1d). Elsewhere total nitrate concentrations were at or close to annual minimum concentrations (Radach and Gekeler, 1996; Radach and Patsch, 1997). The distribution of NO_2 was similar to total nitrate, but concentrations were lower, ranging from <0.01 to 0.39 μmol L^{-1} and averaging 0.03 ± 0.06 μmol L^{-1} (Fig. 1e). $Si(OH)_4$ concentrations were higher ranging from 0.13 to 5.75 and averaging 1.03 ± 0.9 μmol L^{-1}. A prominent band of high $Si(OH)_4$ was observed across the southern North Sea (Fig. 1f). PO_4^{3-} concentrations ranged from <0.02 to 1.4 μmol L^{-1} and averaged 0.14 ± 0.22 μmol L^{-1}. The distribution of PO_4^{3-} was patchy with concentrations >0.5 μmol L^{-1} sporadically found through the central and northern North Sea (Fig. 1g).

Total dissolved nitrogen (TDN) concentrations ranged from 3.6 to 18.4 μmol L^{-1} and averaged 6.7 ± 2.0 μmol L^{-1} (Fig. 1h, Table 1). Concentrations were highest in the southern North Sea close to the European coastline. Total dissolved phosphorous (TDP) concentrations ranged from 0.14 to 0.71 μmol L^{-1} and averaged 0.31 ± 0.1 μmol L^{-1}

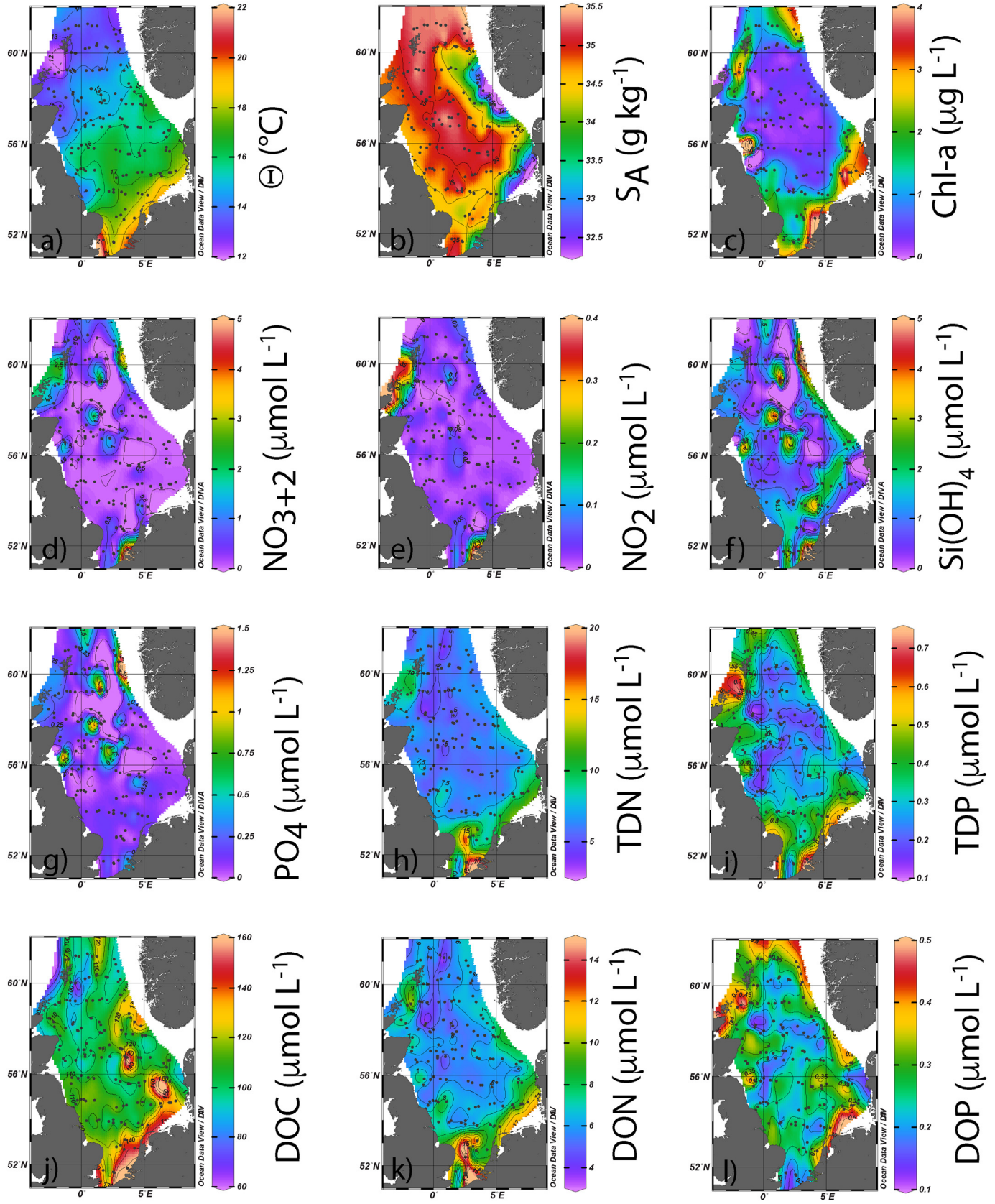

Fig. 1. Regional overview of North Sea surface waters August 2016, including a) Sea surface temperature (conservative temperature), b) Absolute Salinity (S_A), c) Total chlorophyll, d) Total nitrate ($NO_3^- + NO_2^-$), e) Nitrite (NO_2^-), f) Silicate ($Si(OH)_4$), g) phosphate (PO_4^{3-}), h) total dissolved nitrogen (TDN), i) total dissolved phosphorous (TDP), j) dissolved organic carbon (DOC), k) dissolved organic nitrogen (DON), and l) dissolved organic phosphorous (DOP).

Table 1
Summary nutrient concentrations and ranges for the North Sea surface waters August 2016.

	$NO_3^- + NO_2^-$ (μmol L^{-1})	NO_2^- (μmol L^{-1})	$Si(OH)_4$ (μmol L^{-1})	PO_4^{3-} (μmol L^{-1})
Mean ± sd	0.31 ± 0.63	0.03 ± 0.06	1.03 ± 0.93	0.14 ± 0.22
Range	<0.02–4.98	<0.01–0.39	0.13–5.75	<0.02–1.42
	TDN	DON	%DON	%DIN
Mean ± sd	6.74 ± 2.01	6.6 ± 1.77	98.36 ± 3.2	1.64 ± 3.2
Range	3.6–18.4	3.5–16.4	70.8–99.8	0.2–29.2
	TDP	DOP	%DOP	%DIP
Mean ± sd	0.31 ± 0.1	0.26 ± 0.06	86.09 ± 13.41	13.9 ± 13.4
Range	0.14–0.71	0.13–0.46	28.0–97.4	2.6–72.0

(Table 1). Highest concentrations were observed around the periphery of the North Sea (Fig. 1l).

3.4. Organic nutrients

Concentrations of DOC ranged from 61.7 to 185.0 μmol L^{-1} and averaged 108.7 ± 15.7 μmol L^{-1}. Concentrations were highest in the southern North Sea, particularly along the coasts of Belgium and the Netherlands, and lowest (<70 μmol L^{-1}) in the far northwest of the North Sea close to Scotland (Fig. 1j).

DON concentrations ranged from 3.5 to 16.4 μmol L^{-1} (mean 6.6 ± 1.8 μmol L^{-1}; Table 1), with elevated concentrations above 8 μmol L^{-1} in a broad band stretching from the UK to Denmark in the southern North Sea but were generally between 5 and 7 μmol L^{-1} elsewhere (Fig. 1k). A pronounced plume of high DON (>15 μmol L^{-1}) related to the Rhine-Meuse-Scheldt delta was evident but sampling density was insufficient to constrain the spatial extent of the plume, hence the contouring shown in Fig. 1k should be taken as indicative only. DON represented 70.8 to 99.8% (mean 98.4 ± 3.2%) of the TDN pool.

DOP represented 86.1 ± 13.4% of TDP on average but was highly variable contributing between 28.0 and 97.4% of the TDP pool. Concentrations of DOP ranged from 0.13 to 0.46 μmol L^{-1} (mean 0.26 ± 0.06 μmol L^{-1}) and were highest close to the German Bight and near northeast Scotland. Low to intermediate concentrations (0.15–0.35 μmol L^{-1}) were found throughout the central North Sea (Fig. 1l).

The elemental stoichiometry of the organic nutrient pool indicated lower DOC:DON (<15) around the periphery of the North Sea and higher DOC:DON (>17) towards the centre. This indicated both the presence of gradients away from coastal source regions, and differential rates of modification to the underlying DOC and DON pools (Fig. 2a). The Rhine/Scheldt outflow was associated with low DOC:DON (<12) connected to the elevated DON content of these particular sources. More generally, low DOC:DON waters characterised the southern North Sea close to the coast. DOC:DOP distributions were patchy and other than an elevated signal associated with the Rhine/Scheldt outflow, where DOC:DOP exceeded 700:1, no obvious spatial pattern was evident (Fig. 2b). There were strong similarities between the distributions of DOP and DOC:DOP. DON:DOP was largely invariant across the North Sea and generally in the range of 20–30:1 except for a single high DON:DOP plume from the Rhine/Scheldt outflow where DON:DOP exceeded 70:1 (Fig. 2c).

3.5. Spectral absorbance

Summary values of the absorption coefficient at 375 nm (a_{375}), the spectral slope coefficient ($S_{300-600}$) and the slope ratio (S_R), which ranged from 0.09 to 2.74 m^{-1}, 0.005 to 0.027 nm^{-1} and 1.51 to 12.86 respectively, compare well with previous observations from coastal systems (Table 2). A negative correlation was found between $S_{300-650}$ and a_{375} (Fig. 3), similar to that reported by Stedmon and Markager (2001), and which likely reflects conservative mixing between two different source pools (Stedmon and Markager, 2003). No indication of additional source pools was found in the relationship between $S_{300-650}$ and a_{375}, possibly because of the small dataset size, the focus on surface sampling only or the presence of a broadly homogenous organic matter pool during the summer sampling period.

The majority of observations clustered closely together, revealing low variability in a_{375}, $S_{300-650}$ and S_R over much of the North Sea. Notably however, a distinct group of 6 samples measured on consecutive days at the end of the cruise and in a small geographical area southeast of the Fair Isle Channel (~58.2–59.2°N, 2.1°W–1.5°E), revealed high absorption ($a_{375} > 2$ m^{-1}) and low $S_{300-600}$ values (<0.008 nm^{-1}), a characteristic considered indicative of terrestrial inputs (Vodacek et al., 1997; Stedmon and Markager, 2003). Increased salinities (up to 0.27 g kg^{-1} higher), and decreased sea surface temperatures (up to 2.7 °C cooler) coincident with these samples, indicate subtle changes in surface hydrography and are supportive of an influx of North Atlantic water through the Fair Isle Channel (Turrell et al., 1990, 1992), which may have brought with it terrestrial material derived from neighbouring islands. Nevertheless, the changes in spectral signatures

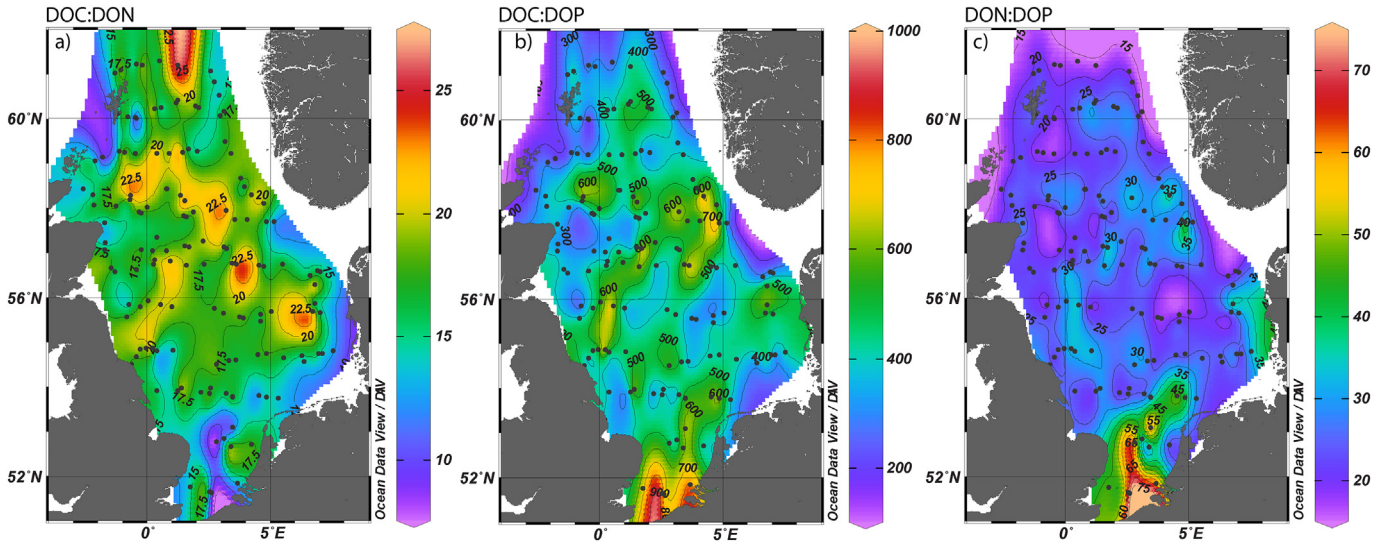

Fig. 2. Stoichiometry of the dissolved organic matter pool, including a) the ratio of DOC to DON, b) the ratio of DOC to DOP, and c) the ratio of DON to DOP.

(increased absorption) and environmental characteristics (increased salinities) are inconsistent with one another if a terrestrial input via freshwater discharge is assumed. The hydrographic changes were certainly not distinct enough from the broad thermohaline range observed throughout the survey to be conclusive of a possible origin, and additional supporting observations were not collected at these latter stations thus there is currently no clear explanation for this observation. Neighbouring stations sampled in the preceding days did not show high absorption indicating either a geographically localized feature or a recent change. Whilst interesting, these 6 stations nevertheless stand apart from the majority of the dataset.

No significant relationship was found between either $S_{300–650}$ or a_{375} and absolute salinity, primarily due to the limited salinity gradient observed (32.3–35.4 g kg^{-1}), but most likely also due to the distance offshore (88% of samples were collected >50 km offshore), which may point against a conservative mixing explanation underlying the relationship between $S_{300–650}$ and a_{375}. However, the absence of relationships at typical oceanic salinities agrees with the findings of Astoreca et al. (2009) who also reported no significant correlation between a_{375} and salinity >34 psu or more generally between the $S_{300–600}$ and salinity. Thus, autochthonous (in-situ) production, photodegradation and/or biodegradation of existing DOM pools is likely to be the dominant source of organic matter present in our samples.

The majority of S_R values were between 2 and 4 (Table 2), with 3 notable but unrelated samples producing $S_R > 5$. With a mean slope ratio of 2.87 ± 1.1 and all estimates of S_R being >1, this tends to support the view that the DOM pool was oceanic and/or extensively photodegraded in origin (Helms et al., 2008; Stedmon and Nelson, 2015).

3.6. Spectral fluorescence

Split-half model validation indicated a 3-component model was the most appropriate representation of the data (core consistency score 85%; Murphy et al., 2013). Sequentially increasing to higher numbers of model components (4–7) resulted in non-validation of the split-half model and a substantial drop in the core consistency score (<61% for 4 components, <12% for 6 components). A 3-component solution is lower than the typical fluorophore content (4–8) reported in comparable marine studies (e.g. Yamashita et al., 2011b), and may indicate underfitting of the PARAFAC model (Murphy et al., 2013). Nevertheless a 3-component model is in agreement with the expected number of fluorophores in a dataset of this size (Murphy et al., 2014b).

Three fluorescent peaks, hereafter fluorophores, were identified via the PARAFAC modeling (Fig. 4a-c). Fluorophore 1 ($\lambda_{ex}/\lambda_{em}$ 245/302 nm) and fluorophore 3 ($\lambda_{ex}/\lambda_{em}$ 270/308 nm; peak B (Coble, 1996; Coble et al., 2014)) are considered to be marine in origin whilst fluorophore 2 ($\lambda_{ex}/\lambda_{em}$ 250/430 nm; peak A) is broadly considered to be terrestrial in origin (Coble, 1996; Stedmon and Markager, 2005; Murphy et al., 2008). Fluorophore 1 was present in all samples but did not correlate with the distribution of chlorophyll. Fluorophore 3 was predominately observed in samples collected along the east coast of the UK (western North Sea) but with a pronounced increase in intensity in the German Bight region of the southern North Sea. Both were regions with high chlorophyll concentrations (>1 mg m^{-3}), though chlorophyll and Fluorophore 3 were not directly correlated. Fluorophore 2 was similarly distributed to fluorophore 3 with peak intensities around the margins of the North Sea, particularly the German Bight, and with the Elbe and Weser rivers and the Baltic Sea outflow being prominent sources of this particular fluorophore (Fig. 5).

3.7. Spectra identification and $SUVA_{254}$

A statistical comparison of spectra with the "OpenFluor" database of fluorescent organic matter spectra identified previously reported spectra for all 3 fluorophores reported here (Fig. 4d-f). Matched components were identified via a 95% similarity criterium and assessed with "Tucker's Congruence Coefficient" via the database (www.openfluor.org; Murphy et al., 2014a, b). Fluorophore 1 was matched with an amino-acid like DOM spectra reported by Jørgensen et al. (2011), and identified in that study as similar to the pure spectrum of the amino acid phenylalanine (Yamashita and Tanoue, 2003). This is considered an unusual spectrum to observe in seawater, as phenylalanine fluorescence is quenched in the presence of tyrosine (Lakowicz, 2006; Yamashita et al., 2008; Jørgensen et al., 2011). Fluorophore 2 was matched with 16 previous datasets, which all of the originating studies considered to be indicative of terrestrial humic material (Peak A in the nomenclature of Coble, 1996; Walker et al., 2009; Osburn and Stedmon, 2011; Yamashita et al., 2011a; Cawley et al., 2012; Graeber et al., 2012; Osburn et al., 2012; Murphy et al., 2013; Yamashita et al., 2013; Bianchi et al., 2014; Shutova et al., 2014; Gonçalves-Araujo et al., 2015). Fluorophore 3 was similar to tyrosine-like DOM fluorescence, has been widely reported for marine waters and is indicative of recent biological activity (Murphy et al., 2011; Yamashita et al., 2011a, 2013; Peak B in the naming scheme of Coble, 1996).

The split-half validated 3-component PARAFAC model did not resolve a terrestrial fulvic acid signature (otherwise known as Peak C; Coble, 1996), and the normalised trace of fluorescence intensities was rather flat in the typical wavelength region for fulvic acids ($\lambda_{ex}/\lambda_{em}$ 320–360/420–460 nm; Fig. 4e). This may be due to the tendency for the position of peak C to shift towards shorter excitation and emission wavelengths (blue-shifted) with increased distance from freshwater sources (Coble, 1996). As the majority of samples were collected >50 km from the nearest land, and as all values of S_A were >32.3 g kg^{-1} it is possible that the terrestrial material represented by fluorophore 2 was aged, degraded and both spectrally and chemically altered from its original composition. Such a scenario supports the inference of (photo) degradation obtained from the elevated values of S_R (Table 2). Furthermore, different contributions of fulvic and humic acid fractions are known to alter the slope coefficient (Warnock et al., 1999) and

Table 2
Mean and range of the absorption coefficient at 375 nm (a_{375}), the spectral slope coefficient ($S_{300–650}$) and the slope ratio (S_R) as measured in this study and in comparison to the literature.

	Absorption coefficient a_{375} [m^{-1}]	Spectral slope coefficient $S_{300–650}$ [nm^{-1}]	Slope ratio S_R	UVA slope ($S_{275–295}$) [nm^{-1}]	UVB slope ($S_{350–400}$) [nm^{-1}]	Source
Mean ± s.d.	0.572 ± 0.518	0.015 ± 0.004	2.87 ± 1.1	0.021 ± 0.007	0.008 ± 0.003	This study
Range	0.089–2.736	0.005–0.027	1.51–12.86	0.005–0.061	0.002–0.014	This study
Range	1.07–1.42	0.0219–0.0255				Kowalczuk et al., 2006
Range		0.016–0.023[a]				Warnock et al. (1999)
Range	0.2–4.29	0.01–0.023[b]				Astoreca et al. (2009)
Range		0.012–0.02[c]	0.7–2.52			Helms et al. (2008)
Range	0.41–7.92	0.017–0.03[d]				Meler et al. (2016)

[a] Based on wavelength range of 250 to 600 nm.
[b] Based on wavelength range of 350 to 500 nm.
[c] Based on wavelength range of 300 to 700 nm.
[d] Based on wavelength range of 300 to 600 nm.

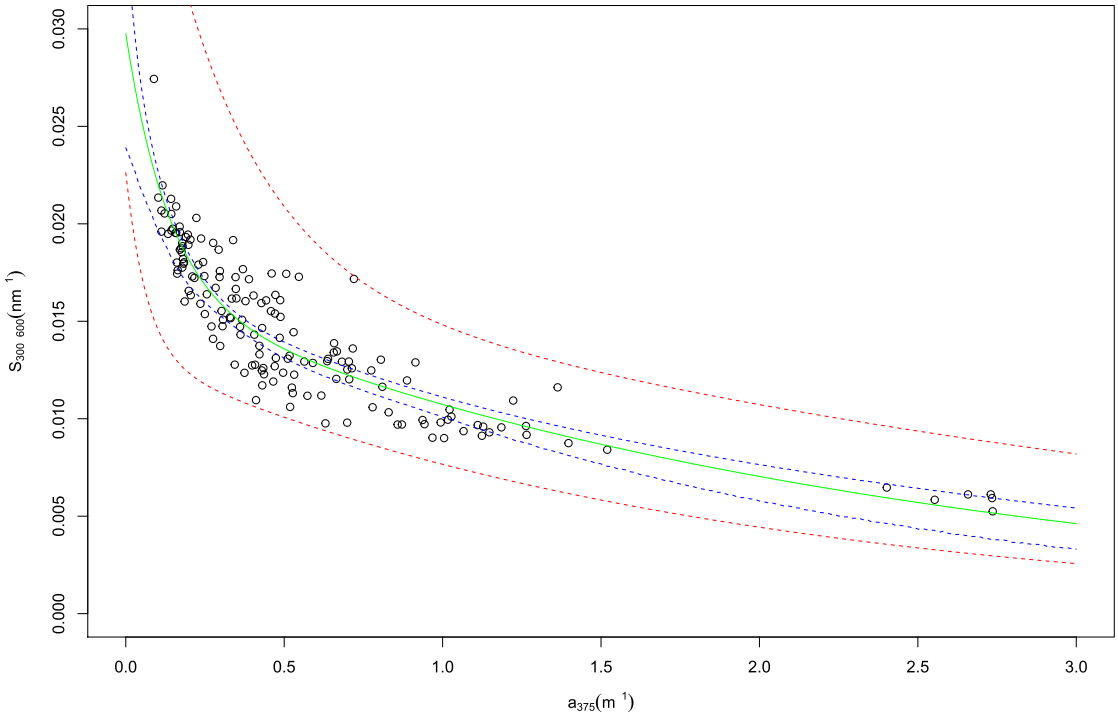

Fig. 3. Relationship between the attenuation coefficient (a_{375}) and the spectral slope ($S_{300–600}$). The green line represents the double exponential best fit to the data ($y = a\ exp.^{(-a_{375}/b)} + c\ exp.^{(-a_{375}/d)}$) where a, b c and d are best fit parameters (a = 0.01634, b = 2.37551, c = 0.01342, d = 0.13695). The red dashed line indicates the 95% confidence interval for the fit parameters whilst the blue line represents the 95% confidence interval for fitted values based on a Monte Carlo simulation. (For interpretation of the references to colour in this figure legend, the reader is referred to the web version of this article.)

changes to $S_{300–600}$ are indicative of changes in DOM composition (Kowalczuk et al., 2006).

$SUVA_{254}$ ranged from 0.55 to 4.42 $m^2\ g^{-1}C$ (mean ± s.d. 1.36 ± 0.65 $m^2\ g^{-1}$ C) with a spatial distribution that was both distinct from the distribution of individual fluorophores or from salinity, but nevertheless shared some similarities (Fig. 5d). In general, $SUVA_{254}$ was elevated around the margins of the North Sea, particularly off northeast Scotland, and reduced towards the central North Sea. The higher DOC aromaticity inferred by higher $SUVA_{254}$ around the margins of the North Sea provides additional support for tDOM input to these waters.

3.8. Spectra relationships to the North Sea environment

Fluorophores 1 and 3 did not correlate with salinity, suggesting that both were of marine origin thus supporting results based on the values of a_{375} and $S_{300–600}$. The intensity of fluorophore 2 was negatively correlated with salinity, supporting the identification and origin of fluorophore 2 as terrestrial humic material (Fig. 6a). The presence of distinct negative relationships within the dataset revealed the presence of two different sources for this humic material, despite similar spectral characteristics. These two sources were broadly identified as river-fed coastal waters around the periphery of the North Sea and the Baltic Sea outflow (Fig. 6a, b). Humic material from both sources became indistinguishable once salinities reached typical oceanic salinities of ~35 g kg^{-1}. Higher DON (>7 μmol L^{-1}) and DOC concentrations (>120 μmol L^{-1}) were generally found at the lowest salinities/highest fluorescent intensities measured, suggesting a low salinity (presumably riverine) source of organic nutrients (Fig. 6c, e), although the same was not true of DOP concentrations, which were more variable with salinity (Fig. 6d), possibly indicating a marine source or sources.

Average values for selected parameters for the three groupings of data indicated in Fig. 6a are shown in Table 3. Small differences in the mean values of $S_{300–600}$, a_{375} and S_R separate the three groups of stations, though the range in values of a_{375} is larger in the North Atlantic grouping than elsewhere. Differences in the mean values of S_A were distinct enough to highlight the low salinity of the Baltic Sea outflow, but the range of salinities within group 1 (coastal) and group 2 (Baltic outflow) were comparable. The highest salinities (>35 g kg^{-1}) were restricted to North Atlantic influenced stations (group 3). Concentrations of DON and DOC were highest in the near coastal waters of the North Sea (group 1), intermediate for the Baltic Sea influenced stations (group 2) and lowest in the North Atlantic influenced stations (group 3). Mean DOP concentrations, however, were similar for all 3 groups.

Marine fluorophores 1 and 3 showed no correlation with any measured parameter, including organic nutrients, inorganic nutrients or chlorophyll concentrations. Fluorophore 2 was significantly and positively correlated with the concentrations of DON ($R^2 = 0.33$, $p < 0.0001$) and DOC ($R^2 = 0.34$, $p < 0.0001$) (Fig. 7a, c) but the correlation with DOP, though statistically significant, was considerably weaker and essentially random ($R^2 = 0.05$, $p < 0.05$) Fig. 7b).

3.9. Land to ocean gradients

To better understand the fate of tDOM in the ocean and the length scales over which terrestrial influences dissipate gradients as a function of distance from land were derived and are shown in Fig. 8. Absorbance measurements revealed a tendency for the spectral slope ($S_{300–600}$) to increase, and absorption coefficient (a_{375}) to decrease with distance offshore (Fig. 8a, b). $S_{300–600}$ reached a local minimum 25–50 km offshore but was also highly variable in this distance interval and overall increased by 0.0016 nm^{-1} from nearshore (<25 km) to offshore (>300 km) waters. In contrast a_{375} displayed a local maximum 25–50 km offshore (0.856 ± 0.790 m^{-1}) and was also highly variable in this interval but otherwise decreased by ~0.21 m^{-1} from nearshore to offshore waters. The slope ratio (S_R) increased offshore by 0.9963 units which

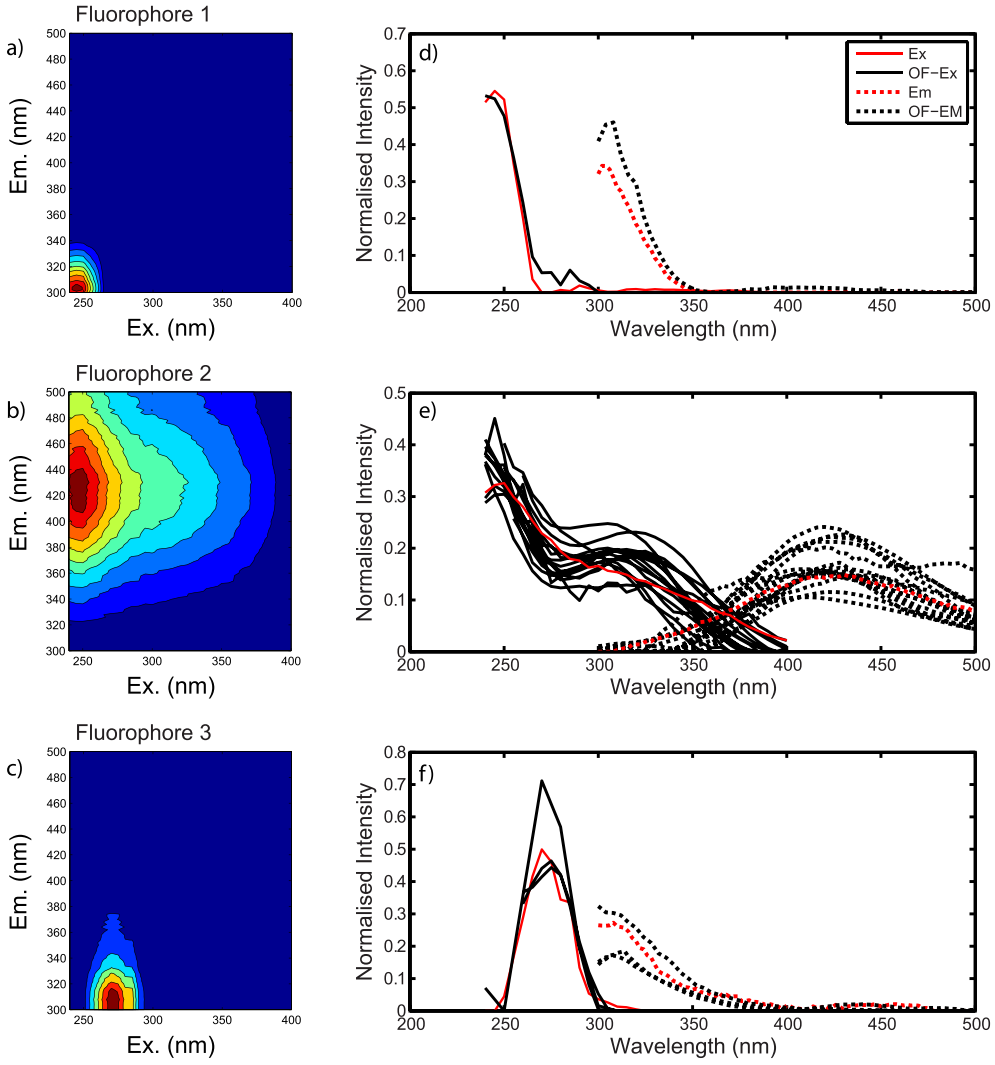

Fig. 4. Results of the PARAFAC modeling and comparison to the OpenFluor database a) spectral fingerprint of fluorophore 1, b) spectral fingerprint of fluorophore 2, c) spectral fingerprint of fluorophore 3, d) Matched comparison of fluorophore 1 to the OpenFluor database, e) Matched comparison of fluorophore 2 to the OpenFluor database and f) Matched comparison of fluorophore 3 to the OpenFluor database.

may indicate a compositional change in the DOM pool and a shift from high to low molecular weight organic matter (Fig. 8c; Helms et al., 2008).

All identified fluorophores displayed a seaward gradient, but the patterns were not consistent (Fig. 8d). The normalised fluorescent intensity of Fluorophore 1 peaked between 50 and 100 km offshore but there was no difference in mean fluorescent intensities between near coastal (<25 km) or offshore (>300 km) waters. Fluorophore 2 was broadly stable at distances up to 200 km from land before decreasing sharply. Fluorophore 3 displayed a pronounced peak (with large variance) between 50 and 200 km offshore but with little difference between near coastal and further offshore waters. As reported previously by Murphy et al. (2008) these patterns are consistent with the gradual removal, or conservative mixing, of (terrestrial) humic-like fluorescence with (oceanic) amino acid-like fluorescence offshore. In particular, the increasing spectral slope ($S_{300-600}$) and decreasing absorption (a_{375}) with distance offshore are expected traits, when terrestrial signatures are replaced with oceanic signatures, and the offshore increase in S_R is indicative of a photochemical transformation within the DOM pool (Helms et al., 2008); an assumption borne out by the positive relationship between S_R and distance offshore (Fig. 8c).

S_A (Fig. 8e) and Θ (Fig. 8f) were variable across all distance intervals examined but both mean values for S_A and Θ tended to increase and become less variable offshore. S_A increased from a mean of 34.498 ± 0.718 g kg^{-1} at <25 km distance from shore to 35.012 ± 0.290 g kg^{-1} at distance >300 km from shore, a relative increase of 0.514 g kg^{-1}. Similarly, mean Θ increased from 14.68 ± 3.47 to 15.29 ± 0.76 °C, an apparent warming of 0.61 °C.

Ratios between the various fluorophores increased with distance from land (Fig. 8g) due to changes in the balance between oceanic and terrestrial ((F1 + F3):F2) fluorophores and a gradual reduction in fluorophore 2 intensity offshore. $SUVA_{254}$ tended to reduce with distance offshore in a comparable manner to a_{375} (Fig. 8h). The offshore gradient in $SUVA_{254}$ was distorted by increased variability in the 25–50 km interval but nevertheless was indicative of reduced aromaticity and associated compositional change in the bulk DOM pool with distance from land, comparable to the inference obtained from the offshore gradient in S_R (Fig. 8c). Offshore gradients were clearly visible in the nutrient fields and sharp reductions in $Si(OH)_4$, $NO_3^- + NO_2^-$ and PO_4^{3-} within 50 km were prominent features of the data (Figs. 8i, j, k). TDN and DON concentrations decreased offshore and were tightly coupled due to DON representing the majority (84–99%) of the TDN pool across

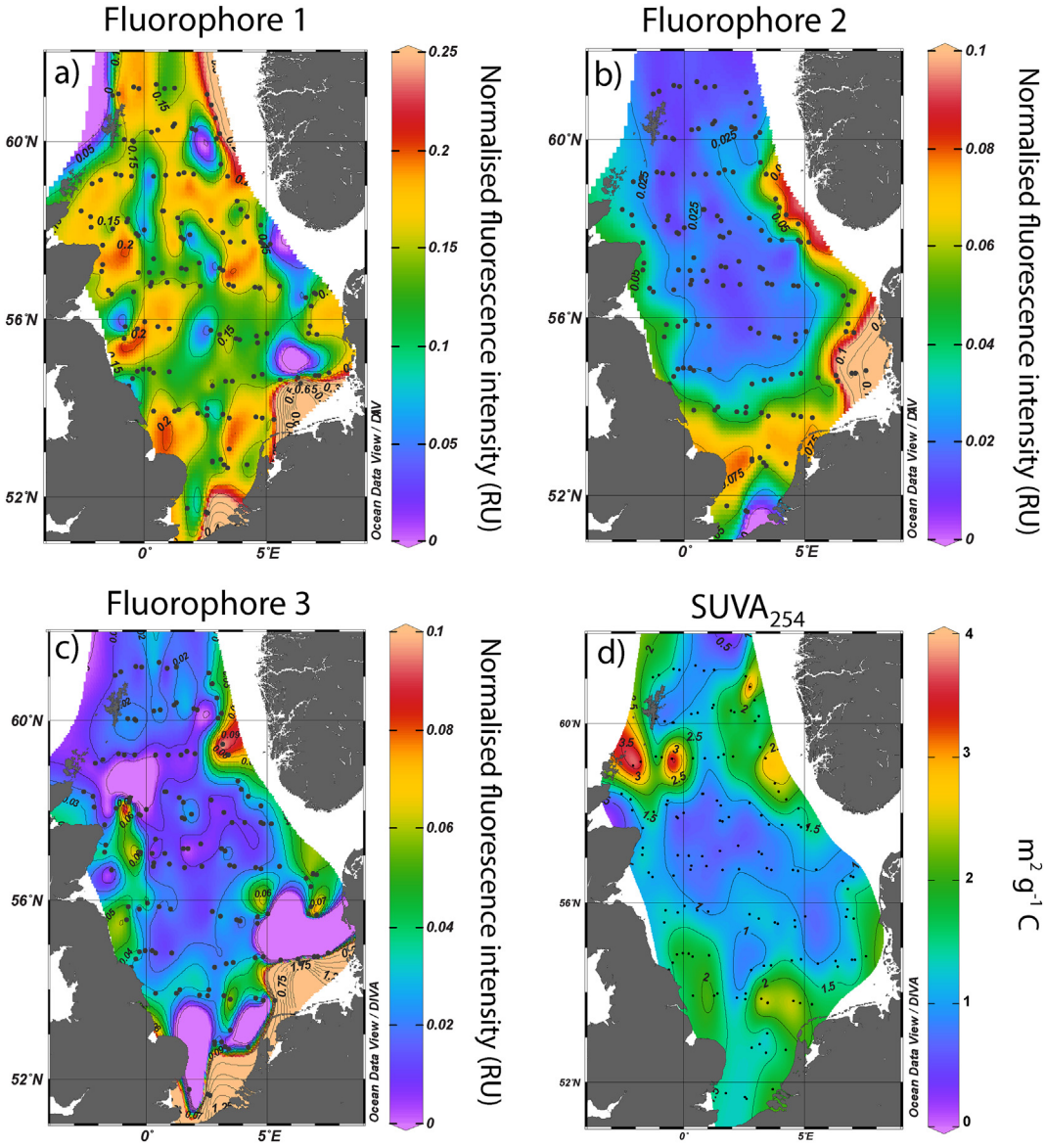

Fig. 5. Maps showing the spatial distribution of a) fluorophore 1 (phenylalanine-like organic matter), b) fluorophore 2 (terrestrial humic organic matter), c) fluorophore 3 (tyrosine-like organic matter) and d) $SUVA_{254}$.

all distance intervals. Within the first 25 km from the coast however total nitrate represented 18.5% of the TDN pool, decreasing to <5% of the TDN pool at greater distances offshore (Fig. 8j). Mean TDP concentrations decreased sharply offshore from ~0.5 μmol L^{-1} at distances <25 km to ~0.27 μmol L^{-1} at distances >300 km offshore. The coupling between TDP and DOP pools was weaker than for the TDN and DON pools due to phosphate representing between 7.6% (>300 km offshore) and 48.6% (<25 km offshore) of the TDP pool (Fig. 8k). DOC concentrations also decreased offshore from ~120 μmol L^{-1} at distances <25 km to ~104 μmol L^{-1} at distances >300 km offshore, a reduction of ~15%. DOC concentrations also generally became less variable with distance offshore (Fig. 8l).

4. Discussion

This study revealed the Rhine-Meuse-Scheldt delta to be a major source of NO_3^- and DON to the southern North Sea. In contrast, the Weser and Elbe rivers and the Baltic Sea outflow were sources of DON but not NO_3^- (Fig. 1). Off northern Scotland DON and NO_3^- concentrations were elevated though the exact source was unclear. Previously, Woodward and Owens (1990) measured elevated NO_3^- concentrations in this region during summer and postulated island induced upwelling of nutrient rich water around the Shetland Islands as a causal mechanism. The Rhine-Meuse-Scheldt delta was also a modest source of PO_4^{3-} but not DOP. In comparison, the Weser/Elbe and Baltic Sea outflows were a significant source of DOP but not PO_4^{3-}. Elevated concentrations of PO_4^{3-} and DOP were observed around Northern Scotland, possibly due to upwelling or North Atlantic inflows collecting tDOM from neighbouring islands or from the Scottish mainland. DOP concentrations mapped onto the correlation between salinity and fluorophore 2 (Fig. 6d) did not distinguish either the Baltic Sea outflow or the Weser/Elbe discharge as distinct sources of DOP to the North Sea. This may relate to significant and ongoing efforts to limit P discharges from agro-industrial and urban activities over recent decades (Radach, 1998; OSPAR Commission, 2003, 2008). Nevertheless, agro-industrial activities largely explain the high PO_4^{3-} discharges associated with the Rhine, Scheldt and Thames rivers to the southern regions of the North Sea, despite overall reductions in P discharges in recent decades

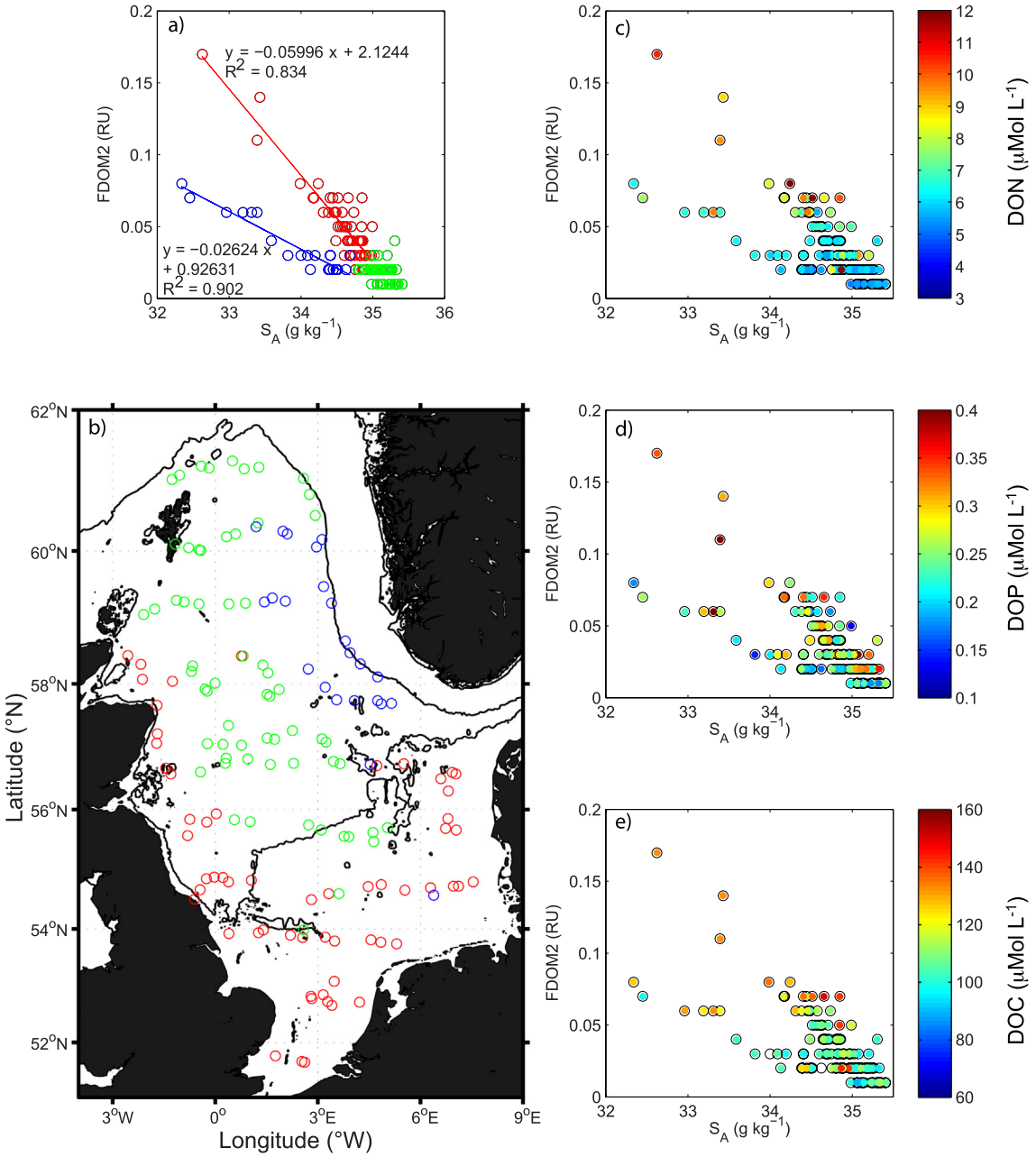

Fig. 6. a) Relationships between fluorophore 2 (terrestrial humic) and salinity with symbols coloured to denote groupings of data corresponding to Baltic outflow (blue), river-fed coastal waters (red), and North Atlantic influenced stations (green), b) Map showing the distribution of each sub-group with the same colouring as in panel a, c) Relationship between fluorophore 2 and salinity and DON, d) Relationship between fluorophore 2 and salinity and DOP, e) Relationship between fluorophore 2 and salinity and DOC. Regression equations in panel a relate to the Baltic outflow (blue) and river-fed coastal waters (red). (For interpretation of the references to colour in this figure legend, the reader is referred to the web version of this article.)

(OSPAR Commission, 2008, 2016). Qualitatively, a stronger similarity existed between the distribution of DOP and chlorophyll than between DOP and salinity (Figs. 1c) suggesting that DOP was released by marine primary production and that the advection of DOP within the high salinity North Atlantic waters entering the North Sea from the north was less important for the overall DOP budget.

The distribution of DOC was similar to the distribution of DON, with highest concentrations found in the shallow southern North Sea. The highest DOC concentrations were generally coincident with the strongest intensity of fluorophore 2, and often co-located with high DON or DOP concentrations. Nevertheless, whilst qualitatively similar to the distribution of fluorophore 2, correlations between fluorophore 2 and the organic nutrients were modest at best (Fig. 7). The distribution of DOC and DON, and to a lesser extent DOP, could not therefore be considered directly indicative of terrestrial inputs.

Correlations between salinity and the normalised intensity of terrestrial fluorophore 2 clearly showed a distinction between the high fluorescence yield associated with low salinity waters from the Elbe/Weser outflow, and the low fluorescence yield associated with the low salinity outflow from the Baltic Sea (Fig. 6). The linearity of both negative correlations suggests that the spectral signature of individual source waters was eventually lost through conservative mixing with oceanic waters, rather than by non-conservative biotic or abiotic removal processes. The difference in fluorescence intensity between these two sources likely relates to compositional or concentration differences in tDOM with the ~30 year residence time of the Baltic (Voss

Table 3
Mean ± s.d. and range of selected parameters based on the 3 groupings of stations indicated in Fig. 6a.

Group		Absorption coefficient a_{375} [m^{-1}]	Spectral slope coefficient $S_{300-650}$ [nm^{-1}]	Slope ratio S_R	S_A [$g\ kg^{-1}$]	DON [$\mu mol\ L^{-1}$]	DOP [$\mu mol\ L^{-1}$]	DOC [$\mu mol\ L^{-1}$]
1 (coastal)	Mean	0.0152 ± 0.0027	0.5063 ± 0.2509	2.9179 ± 1.5695	34.5615 ± 0.4273	7.57 ± 2.2	0.27 ± 0.06	117.08 ± 16.68
	Range	0.01–0.021	0.159–1.363	1.5149–12.8566	32.6243–34.99	5.39–16.36	0.13–0.45	95–185
2 (Baltic)	Mean	0.0145 ± 0.0037	0.5883 ± 0.4037	2.731 ± 0.5568	33.9438 ± 0.6919	6.25 ± 0.98	0.23 ± 0.06	109.72 ± 12.55
	Range	0.009–0.02	0.17–1.397	2.0222–4.4621	32.3395–34.6786	4.51–9.63	0.13–0.42	96.67–132.5
3 (N. Atlantic)	Mean	0.0149 ± 0.0045	0.4764 ± 0.5601	2.9303 ± 0.7054	35.1265 ± 0.1499	5.82 ± 0.94	0.26 ± 0.06	100.57 ± 10.92
	Range	0.005–0.027	0.089–2.736	1.8219–5.3562	34.7999–35.4069	3.52–9.41	0.15–0.46	61.67–142.5

et al., 2011) likely providing time for significant microbial and photochemical breakdown of tDOM compared to the riverine inputs, which are of more recent origin. Differences between source regions are important for the overall interpretation of the fluorescent spectra, and in addition to the age of material, drainage through known peat regions can have a significant impact on the chemical character of tDOM, for example in discharge from the Elbe river (Laane and Kramer, 1990) or some of the larger British rivers draining to the North Sea such as the Humber (Eatherall et al., 1998; Worrall and Burt, 2007).

4.1. North Sea tDOM distribution

The three fluorophores identified in this study were all successfully cross-referenced to the OpenFluor database (Murphy et al., 2014a, b). Fluorophore 2 appears as a common fluorophore in the database and is widely linked to terrestrial material. Whilst the presence of negative correlations between fluorophore 2 and salinity support a terrestrial origin (Fig. 6), other spectral characteristics, such as S_R, were less emphatic in their classification of a terrestrial origin, instead implying significant photochemical reworking of organic matter and/or mixing of tDOM with oceanic DOM. It is probable that the spectral fingerprint of fluorophore 2 was significantly altered from that of fresh terrestrial material, particularly given the offshore decrease in $SUVA_{254}$ (Fig. 8h). The distribution of fluorophore 2 may not, in this case, be useful in tracing recent terrestrial inputs to the coastal zone, though the relationship to salinity (Fig. 6) indicates a longer-term use in identifying the mean spatiotemporal distribution of tDOM inputs. More interestingly, the distribution of fluorophore 2 was almost identical to the map of natural fluorescence intensity reported for the North Sea by Laane and Kramer (1990) (Fig. 9). This similarity suggests that the distribution of both bulk FDOM and of specific fluorescent compound classes (such as represented by fluorophore 2) may be broadly stable in time, as the two datasets were collected over 30 years apart (1985 and 2016). Laane and Kramer (1990) also argued for the spatiotemporal stability of North Sea FDOM fields, after comparing their observations to fluorescent data presented by Kalle (1956), and finding little difference between the 1950s and 1985. Thus, the spatial distribution of fluorophore 2 shown in Fig. 5b may be a persistent feature of the North Sea with observations supporting the stability of this distribution extending back to the 1950s (Kalle, 1956; Laane and Kramer, 1990). This is somewhat surprising given the near-doubling of DOC concentrations observed in many rivers draining the UK and Fennoscandia (Monteith et al., 2007; Kritzberg and Ekström, 2012; Räike et al., 2012, 2016), suggesting that any changes in freshwater DOM loadings to marine systems have been insufficient to change observed concentrations at the scale of the North Sea. Fluorophore 2 may be useful for identifying the mean long-term distribution of terrestrial material within the North Sea. As such, the rapid decrease in intensity of fluorophore 2 at distances >200 km offshore (Fig. 8d) may hint at a key region for future research into the processes limiting tDOM transference from this shelf system to the wider North Atlantic Ocean.

Despite the apparent stability of the fluorescent organic matter field, Osburn and Stedmon (2011) recently drew attention to the lack of associated lignin biomarkers within the terrestrial fluorophores in the Southern North Sea, arguing for a more complex story than simple riverine input and subsequent coastal mixing. Optical measurements such as a_{375}, $S_{300-600}$ and S_R all indicate marine or substantially aged and photodegraded tDOM was present during the survey (Table 2). This is in agreement with the limited salinity gradient observed, which did not include fresh water end member measurements (all samples > 32 $g\ kg^{-1}$). Notably, however, photodegradation of lignin, and of chromophoric or coloured DOM (CDOM), and of DOM more generally, can be rapid, with 75% of dissolved lignin removed in <1 month (Opsahl and Benner, 1998; Benner and Kaiser, 2011), and >50% of CDOM lost in <2 months (Moran et al., 2000). The lack of strong lignin biomarker concentrations in the southern North Sea does not undermine the argument of riverine input as the dominant source, but does support a conclusion of this study that the observed terrestrial

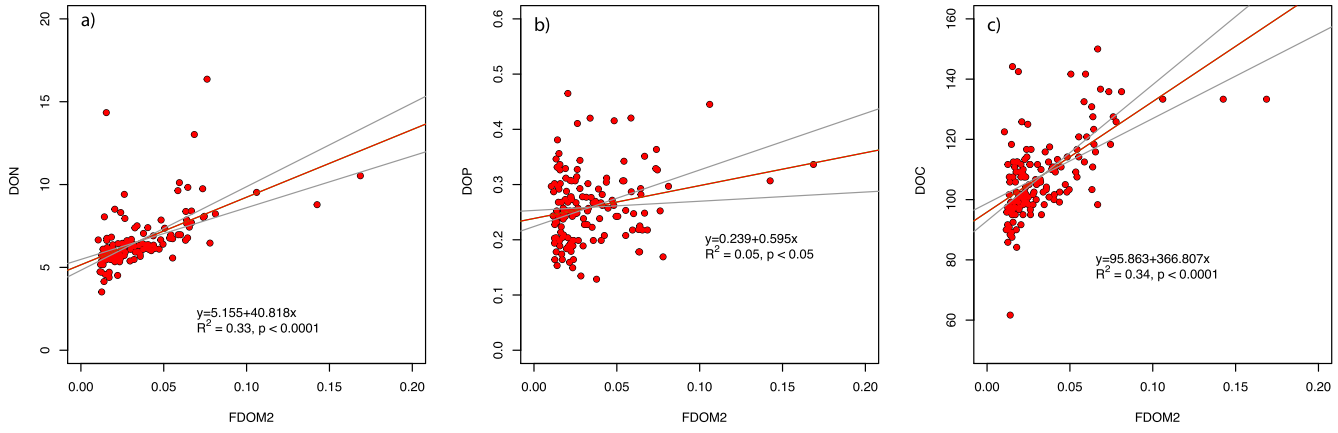

Fig. 7. Regression results between a) fluorophore 2 and DON, b) fluorophore 2 and DOP, c) fluorophore 2 and DOC. Red lines indicate line of best fit, grey lines the 95% confidence intervals for the best fit lines. (For interpretation of the references to colour in this figure legend, the reader is referred to the web version of this article.)

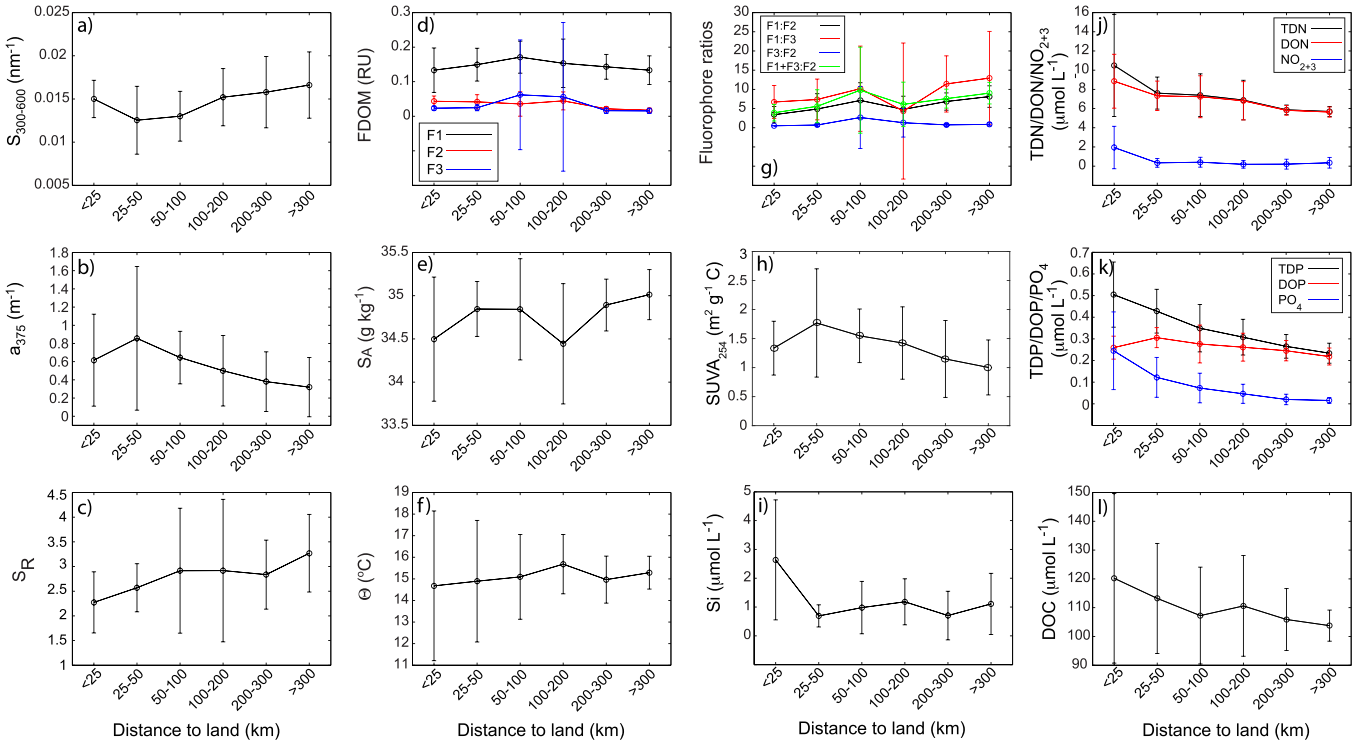

Fig. 8. Relationship between selected measured parameters and distance from land including a) absorption spectral slope ($S_{300–600}$), b) absorption coefficient at 375 nm (a_{375}), c) slope ratio (S_R), d) normalised fluorophore intensity, e) absolute salinity (S_A), f) conservative temperature (Θ), g) fluorophore ratios, h $SUVA_{254}$, i) silicate, j) dissolved nitrogen species, k) dissolved phosphorous species, l) dissolved organic carbon.

fluorophore is largely of non-recent origin and thus likely to be refractory in nature; an observation further supported by the distribution of $SUVA_{254}$ (Fig. 5d).

4.2. tDOM distribution relative to riverine inputs

A recent global synthesis by Dai et al. (2012) of riverine DOC inputs to the ocean included descriptions of 9 rivers entering the North Sea. The mean annual riverine DOC fluxes ranged from 0.014 Tg C yr^{-1} (river Tweed, UK) to 0.204 Tg C yr^{-1} (river Rhine, The Netherlands). The two largest drainage areas of the sites considered by Dai et al. are the Rhine (0.165×10^6 km^2) and the Elbe (0.124×10^6 km^2), with corresponding discharges of 70.5 and 21.4 km^3 yr^{-1}. Both rivers enter the North Sea in the southern or southeastern sector and the outflows are close to the region of highest intensity for fluorophore 2 (Fig. 10). Interestingly, neither the Rhine nor the River Elbe are characterised by high DOC concentrations or drainage area averaged DOC fluxes (242 and 383 μmol C L^{-1} or 1.2 and 0.8 g C m^{-2} yr^{-1} respectively), indicating that both rivers are comparatively dilute DOC sources. Instead, the highest DOC concentrations were reportedly for the Tyne river (UK, 1230 μmol C L^{-1}/9.5 g C m^{-2} yr^{-1}) and the Scheldt (the Netherlands, 567 μmol C L^{-1}/1.2 g C m^{-2} yr^{-1}) or Ems rivers (Germany, 567 μmol C L^{-1}/2.2 g C m^{-2} yr^{-1}) (Dai et al., 2012). A weak fluorophore signature was observed offshore of the Tyne outflow (~55°N; Fig. 10), most likely due to the comparatively low annual discharge of 1.4 km^3 yr^{-1} despite the highest DOC production rate per unit of land area. There was little indication of elevated fluorescent intensities immediately offshore of the Scheldt, but the Ems river may contribute to the overall distribution of fluorophore 2 by virtue of the location of the river mouth lying midway between the Rhine and Elbe rivers. Annual DOC discharges were 0.021, 0.026 and 0.018 Tg C yr^{-1} for the Tyne, Scheldt and Ems rivers respectively, with discharges being considerably smaller than reported for the Rhine and Elbe (0.099 Tg C yr^{-1}) rivers (Dai et al., 2012). Thus, despite being concentrated DOC sources, the spatial impact of discharges from the Tyne, Scheldt and Ems rivers seems to be geographically limited.

There are nevertheless limitations to the interpretation of riverine inputs obtainable from Fig. 10, largely due to the limited number of rivers considered but it would seem that a substantial terrestrial signal originates from the east coast of the UK, particularly around East Anglia (~53°N), that is not associated with the 9 rivers indicated in Fig. 10. Several additional rivers, including the Great Ouse (554 μmol DOC L^{-1}/0.23 g C m^{-2} yr^{-1}; Neal et al., 2000), and at least one large estuary, the Wash, enter the North Sea here contributing to the East Anglian plume (Bristow et al., 2013), which could conceivably explain the pattern observed. However, whilst Worrall et al. (2012) have estimated the average annual flux of DOC from the UK to be 0.91 ± 0.35 Tg C yr^{-1}, with a dominant export flux from regions rich in organic soils, such as the highlands of Scotland, only minor fluxes were estimated for the UK's east coast in that study. Furthermore, a qualitative examination of North Sea DOC distributions does not indicate elevated concentrations of DOC off northeast Scotland (Fig. 1), yet the intensity of fluorophore 2 was elevated along the east coast of the UK (Fig. 6). These contrasting results suggest that whilst terrestrial material is reaching coastal waters of the western North Sea and leaving an identifiable spectral fingerprint within the DOM pool, the absence of associated high DOC concentrations indicates rapid dilution of inputs and/or rapid biological and photochemical transformation of tDOM. Interestingly, elevated DOP concentrations were observed around the Orkney Islands and Duncansby Head (northeast Scotland), stretching as far north as the Shetland Islands (Fig. 1), with this signature possibly advected eastwards through the Pentland Firth (the narrow seaway separating mainland Scotland from the Orkney Islands) or northwards from the Moray Firth. The dissimilarity with the distribution of fluorophore 2, however, suggests that the DOP enrichment seen in this region is marine rather than terrestrial in origin.

Low salinity waters along the Belgian, German and Danish coastline have long been recognised (Lee, 1980; Otto et al., 1990; Huthnance,

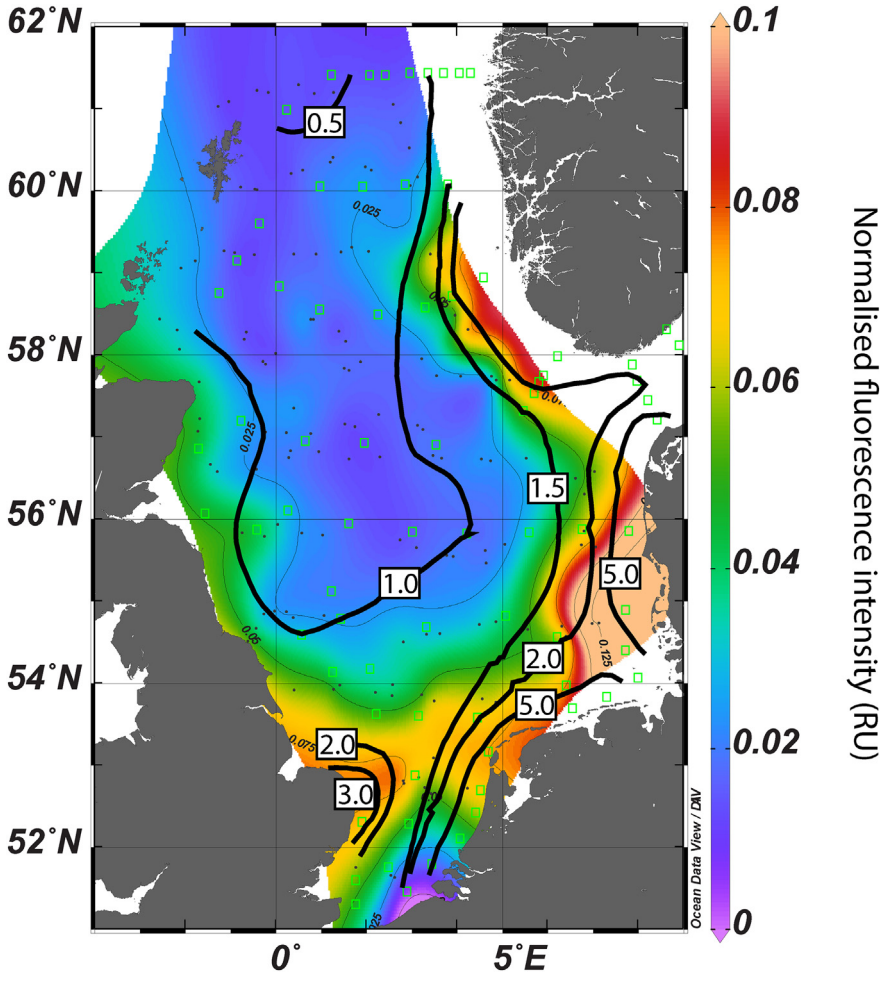

Fig. 9. Comparison of the North Sea natural fluorescence distribution as measured by Laane and Kramer (1990) in the 1980s with the results of this study. Note that the Laan and Kramer contours (thick black lines) are in units of millifluorescence (mFl), whilst fluorophore 2 (thin black lines and underlying contour map) is normalised fluorescence intensity (Raman Units). The green squares indicate the Laane and Kramer sampling positions. (For interpretation of the references to colour in this figure legend, the reader is referred to the web version of this article.)

1991), and are commonly associated with freshwater discharge from the Scheldt, Rhine/Meuse, Elbe and Weser rivers. The Scheldt is a concentrated DOC source (Dai et al., 2012), hence a river of particular interest for organic inputs to the North Sea. Models suggest however, that the influence of the Scheldt discharge on near coastal salinities is geographically limited and the Rhine/Meuse discharge is dominant (Lacroix et al., 2004). Subsequent eastward advection of low salinity waters into the German Bight and then northwards within the Jutland Coastal Current is argued to draw low salinity and DOM rich waters away from the German Bight and into the Kattegat (Stedmon et al., 2010). In the present study, the data indicate the Baltic Sea outflow to be a distinct secondary source of tDOM rather than a recirculatory source of tDOM originating from the German Bight.

4.3. tDOM supply from the Baltic Sea

Drainage basins surrounding the Baltic Sea contain extensive coniferous forests and peatlands with estimates of riverine organic carbon inputs ranging from 2.2 to 3.7 Tg C yr^{-1} (Thomas et al., 2010; Kulinski and Pempkowiak, 2011; Seidel et al., 2017). There is a net export of organic carbon from the Baltic to the North Sea of between ~1.7 and ~3.5 Tg C yr^{-1} (Kulinski and Pempkowiak, 2011; Gustafsson et al. 2014; Seidel et al., 2017). However, Bianchi et al. (1997) reported north to south gradients in lignin concentrations from the northern Bothnian Bay to the Baltic Proper revealing rapid reduction in lignin concentrations with distance from the input sources. The long residence time of the Baltic Sea also provides time for dilution via mixing, and for substantial microbial reworking and photodegradation of tDOM before water exits the Baltic Sea via the Skagerrak into the North Sea (Seidel et al. 2017). Once released from the Skagerrak transport times to the northern boundary of the North Sea (~62°N) are approximately 2 to 6 weeks (Føyn and Rey, 1981); hence Baltic Sea inputs may not persist in the North Sea for very long. In contrast, the Weser and Elbe outflow to the German Bight have more immediate and substantial loadings of fresh organic material from both natural and anthropogenic origins. In keeping with previous observations reported by Søndergaard et al. (2003), this terrestrial signature is, nevertheless, quickly dissipated in the coastal zone, such that much of the central North Sea appears to be without any terrestrial signature within the DOM pool (Fig. 5). This distribution matches the general circulation of the North Sea and of the North Atlantic inflow patterns. Thus distinct tDOM inputs from the Baltic Sea and from major rivers are required to explain the overall tDOM loading of the North Sea.

4.4. Submarine groundwater discharge and sediment sources of tDOM

Submarine groundwater discharge (SGD) is a significant component of the hydrological cycle and a known source of tDOM and other nutrients in coastal settings (Swarzenski et al., 2007; Moore, 2010). SGD inputs of tDOM can be due to direct inputs from groundwater discharge as well as mobilization of significant terrestrial POC deposition in shallow waters (Burdige et al., 2000) and elevated DOC concentrations in

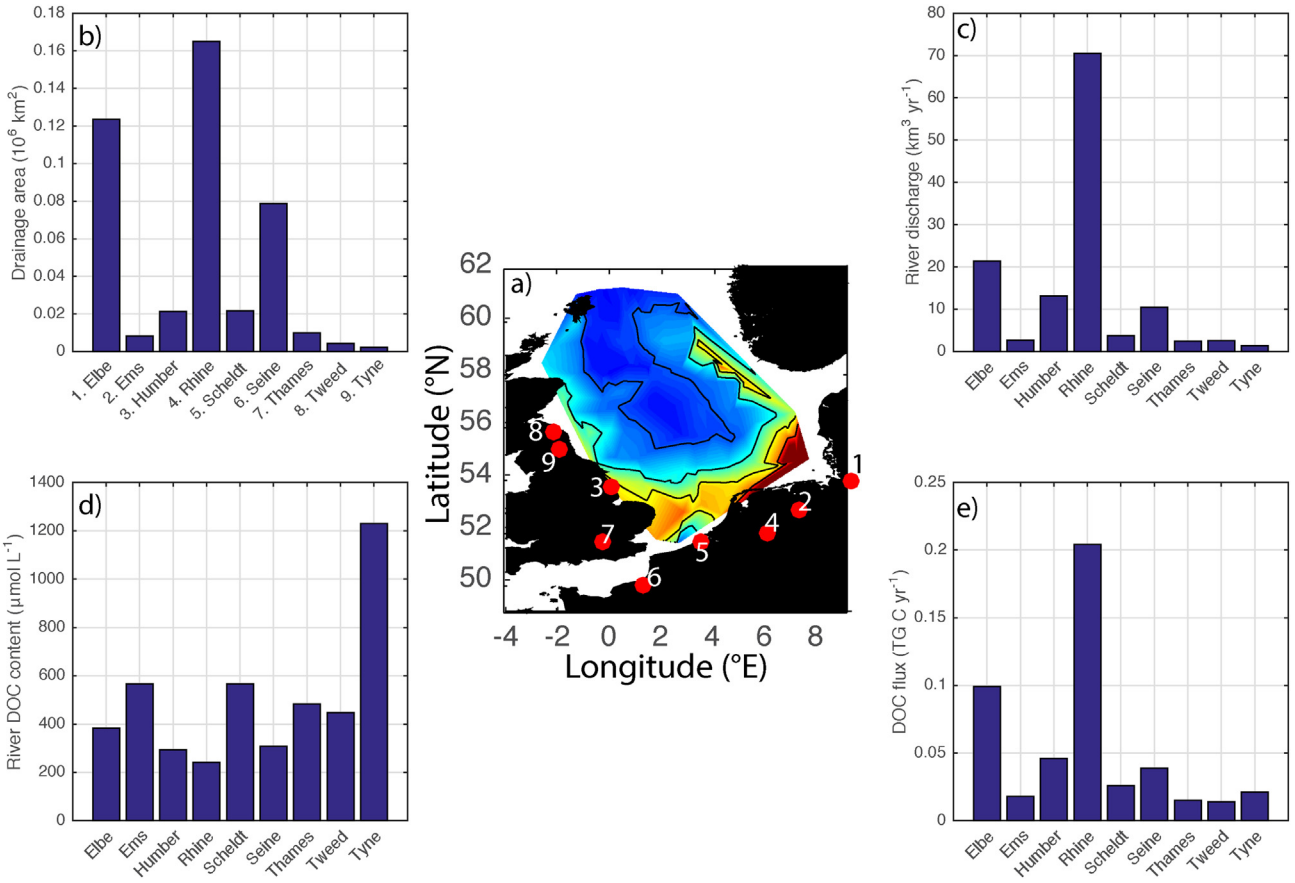

Fig. 10. Summary overview of river inputs to the North Sea as compiled by Dai et al. (2012). a) Map showing river locations in relation to the spatial distribution of fluorophore 2 (terrestrial humic material; Fig. 5b) and b) river drainage area, c), annual mean river discharge, d) mean riverine DOC concentration and e) annual riverine DOC flux. The numbers shown in panel a correspond to the rivers as numbered in panel b.

sediment porewaters due to microbial activity (Lübben et al., 2009; Moore et al. 2011). Permanently well mixed waters in the southern North Sea (Lee, 1980; Lacroix et al., 2004), coupled with observations of significant groundwater discharge in the Wadden Sea area (Lübben et al., 2009; Moore et al., 2011) may make SGD a viable source for some of the observed tDOM signal. In addition, nitrogen and phosphorus concentrations in UK groundwater are elevated compared to coastal waters (Stuart and Lapworth, 2016) and may fertilise and stimulate microbiological processes which release DOC indirectly from coastal sediments (Slomp and Van Cappellen, 2004). Inputs from SGD sources are however considered hard to distinguish due to high background concentrations of tDOM in the German Bight derived from riverine inputs (Stedmon et al. 2010). Nevertheless, sedimentary release and/or microbially reworked DOM exported from intertidal sediments cannot be excluded as potential sources for some of the observed signals seen in coastal areas of the southern North Sea. In particular, high intensities of fluorophore 1 (Fig. 5a) in a region of known groundwater discharge (Lübben et al., 2009; Moore et al. 2011) may indicate a sedimentary origin mobilised by SGD.

4.5. Linear versus non-linear tDOM removal

Salinity induced aggregation is suggested to drive the removal of tDOM at the freshwater-seawater interface (typically at salinities <15 g kg^{-1}; Sholkovitz et al., 1978), along with bacterial reworking and photochemical alteration (Bianchi, 2007). These contrasting processes broadly control the linear or non-linear behaviour of tDOM in coastal waters. The findings reported here suggest that the dual relationships between tDOM fluorescence and salinity for the Baltic and European continental river outflows are linear across the salinity range sampled with no indication of non-linear removal at salinities >32 g kg^{-1} (Fig. 6a). At oceanic salinities the terrestrial signature is weak, and probably weakened further by strong photochemical alteration over seasonal or multiyear timescales. As a consequence of this, and in conjunction with the cyclonic circulation of the North Sea, the signature of terrestrial material is broadly restricted to the edges of the North Sea, where salinities are lower and the distance to terrestrial sources shorter. Such a pattern is also in keeping with estimates of the residence time of the North Sea, which although varying for different sub-sectors, is estimated to be approximately 2 years for the southern North Sea (Prandle, 1984; Blaas et al., 2001). The residence time of water within the North Sea can be extended up to 4 years for waters entering the North Sea near Scotland, or reduced to <100 days for water in the Norwegian Trench (Blaas et al., 2001). Thus, the spectral signature of fluorophore 2 predominately found in the southern North Sea is probably reflective of material that is ~2 years old, and certainly <4 years old.

4.6. Photodegradation versus conservative mixing

The relationship between a_{375} and $S_{300–600}$ (Fig. 3) indicated conservative mixing between two sources waters, a marine component with low a_{375} and high $S_{300–600}$ and a fresher component with high a_{375} and low $S_{300–600}$. In a simple scenario of fresh water input mixing with oceanic water, the resulting relationship would be similar to that shown in Fig. 3, thus the relative proportion of fresh and marine water would dictate the dilution of terrestrial inputs (Stedmon and Markager, 2003). In contrast, the trend for decreased values of a_{375} and increased values of $S_{300–600}$ and S_R with distance offshore (Fig. 8)

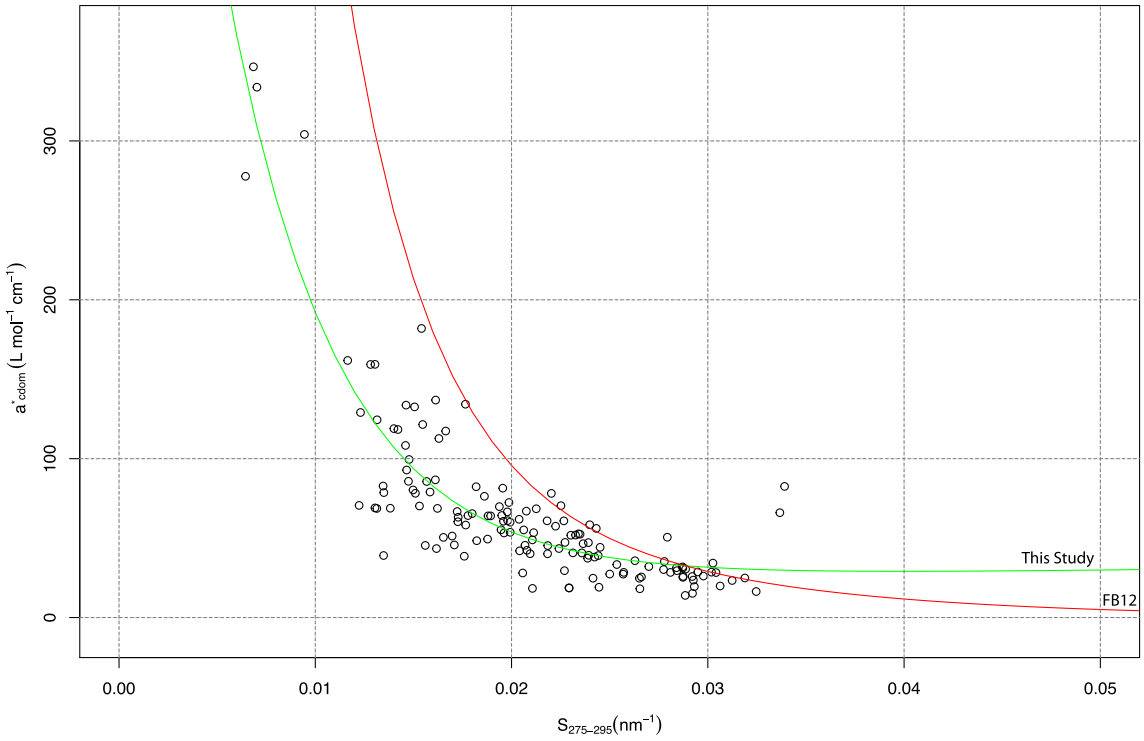

Fig. 11. Relationship between the spectral slope ($S_{275-295}$) and the DOC normalised absorption coefficient at 350 nm ($a^*_{cdom} = a_{350}$/DOC) for the North Sea. The green line represents the double exponential best fit to the data ($a^*_{cdom} = \exp.^{(\alpha-\beta\ S_{275-295})} + \exp.^{(\gamma-\delta\ S_{275-295})}$ where α, β γ and δ are best fit parameters ($\alpha = 3.1390, \beta = -5.0978, \gamma = 6.9050, \delta = 178.2239$). The red line indicates the corresponding fit obtained by Fichot and Benner (2012). (For interpretation of the references to colour in this figure legend, the reader is referred to the web version of this article.)

are also indicative of photodegradation effects (Helms et al., 2008; Fichot and Benner, 2012). Specifically, the offshelf increase in S_R, which was driven by an increase in $S_{275-295}$ and a decrease in $S_{350-400}$ with distance from land, has been linked to coincident shifts in the molecular weight of the DOM pool (Helms et al., 2008). Such gradients fit the conceptual model of the cumulative effects of photodegradation in coastal waters described by Fichot and Benner (2012), and recently demonstrated at the global level by Maasicotte et al. (2017), in which $S_{275-295}$ increases and DOM concentrations and molecular weights decrease along the continuum from river mouth to shelf break. Indeed, a repeat of the analysis described by Fichot and Benner (2012) relating $S_{275-295}$ to the DOC normalised absorption coefficient at 350 nm (i.e. $a^*_{cdom} = a_{350}$/DOC) revealed similar results with low values of $S_{275-295}$ corresponding to high DOC normalised absorption (a^*_{cdom}), and higher values of $S_{275-295}$ corresponding to low DOC normalised absorption (Fig. 11). There were, however, several differences making the identification of riverine (low $S_{275-295}$) or marine (high $S_{275-295}$) end members problematic. Firstly, there was considerably more scatter in the North Sea dataset compared to the Gulf of Mexico dataset studied by Fichot and Benner (2012). This may be due to weaker riverine inputs (due to distance offshore), greater variability in DOC concentrations, larger marine influences (again due to distance offshore) and more generally a narrower salinity range in the North Sea (32.3–35.4 g kg^{-1} vs 0–36.95 psu in Fichot and Benner (2012)). Secondly, whilst the range of a^*_{cdom} was comparable between studies, lower estimates of $S_{275-295}$ were obtained for the North Sea, resulting in a shift of the best fit line (Fig. 11). Thirdly, the Fichot and Benner (2012) relationship converged towards zero a^*_{cdom} at high $S_{275-295}$ values, whilst the North Sea dataset did not. The Fichot and Benner (2012) relationship would therefore imply minimal impact by DOC on absorption at high $S_{275-295}$ values, whereas the North Sea dataset converged towards a constant value of a^*_{cdom} above $S_{275-295}$ values of 0.03 nm^{-1}. Regardless of these differences, which may also reflect regional variation in the relationship between $S_{275-295}$ and a^*_{cdom} (Maasicotte et al., 2017), the general relationship between $S_{275-295}$ and a^*_{cdom} is comparable between these two datasets, and thus supportive of the global utility of the relationship for tracing changes in the lability of tDOM (Maasicotte et al., 2017).

4.7. Pathways for tDOM export to the Atlantic Ocean

Based on the results of this study, and the similarity and long-term stability of terrestrial fluorescence distribution to previous observations (Fig. 9), it appears that terrestrial inputs are restricted to near coastal waters (<200 km from land), largely advected around the edges of the North Sea, and most likely exit the North Sea along the Norwegian coast to the northeast, following the North Sea residual circulation. However, the observed tDOM signal was weak in the northeastern North Sea, where Norwegian coastal waters were not adequately sampled to determine their terrestrial loadings, though they are believed to be high (Højerslev, 1981). Thus, it remains unclear if a route for tDOM export from the North Sea exists closer to Norway than was sampled here or whether the tDOM spectral signature is almost entirely lost through mixing and photodegradation within the confines of the North Sea minimising the potential for tDOM export to the open ocean. The latter scenario would suggest that there is significant potential for the loss of river borne terrestrial carbon to the atmosphere after discharge to the coastal ocean.

4.8. Open questions

Questions remain concerning the age and lability of the identified spectral components, the relative contribution of terrestrial and oceanic DOM to the measured organic nutrient pools, the semi-constant spatial distribution of (terrestrial) fluorescence over 6 decades, the ultimate fate of terrestrial material entering the North Sea, the relative balance between photochemical degradation, microbial breakdown, and export

to the ocean, the role of seasonal variability, and, more generally, the significance of photodegradation as a removal process. These are not new questions and are active areas of research. One intriguing result reported here, was the widespread distribution of phenylalanine-like fluorescence (fluorophore 1). Its ubiquitous presence would indicate a marine origin, though its precise source is unclear. Certainly, there was no distinction between peripheral or central North Sea waters nor any major offshore gradient or relationships to salinity or chlorophyll. Though vascular plants produce lignin phenols from phenylalanine during the lignin biosynthesis phase (Whetten and Sederoff, 1995), the subsequent release and accumulation of phenylalanine in marine waters during the degradation of lignin has not, as far as we are aware, been reported for the ocean, whereas rapid photodegradation of phenylalanine is well recognised, and would act to remove phenylalanine from the water column (Benner and Kaiser, 2011). A strong contender for the origin of this fluorophore may therefore be a blue-shifted tyrosine spectrum of marine origin (Yamashita et al., 2008). Consequently, given the rarity of observations of this fluorophore, a degree of caution is advised against extrapolation to possible sources.

5. Conclusions

- Three fluorophores were spectrally identified in the dissolved organic matter pool of North Sea surface waters during a summer survey. These fluorophores represented 1 terrestrial humic, 1 tyrosine-like amino acid and 1 phenylalanine-like amino acid compound classes.
- Only weak correlations were found between DOC, DON or DOP and the individual fluorophores indicating significant marine contributions to the organic nutrient pools.
- Salinity had the strongest relationship to the humic fluorophore supporting a terrestrial source.
- Two distinct sources of terrestrial fluorophores were identified, the Baltic Sea outflow and the Weser/Elbe rivers but minor contributions from other rivers are required to explain the observed distribution of humic material.
- Fluorophore 1 (phenylalanine-like amino acid) shared spatial similarities to PO_4 and DOP fields, fluorophore 2 (terrestrial humic) was distributed around the edge of the North Sea whilst fluorophore 3 (tyrosine-like amino acid) could not be linked to the distribution of any measured parameter.
- Spectral absorption measurements indicated either aged or oceanic organic matter to be present within the humic fluorophore pool. It did not support fresh tDOM input, suggesting that the observed humic fluorophore was not recently added or had been rapidly photochemically altered.
- The residence time of the southern North Sea (~2 yr) is sufficient to retain tDOM over multi-year timescales, providing adequate time for photodegradation of material and may explain the “aged” absorption results and the offshore gradients in parameters.
- The apparent multi-decadal stability of DOM fluorescence in the southern North Sea suggests that increased tDOM inputs in recent decades have been insufficient to change observed distributions at the scale of the North Sea.
- There was no clear evidence of significant tDOM export from the North Sea to the Atlantic Ocean suggesting that tDOM inputs are remineralized internally with the potential for subsequent loss to the atmosphere. However Norwegian coastal waters were unsampled and an export flux associated with the Norwegian Trench cannot be discounted.

Acknowledgements

We would like to thank the officers and crew of the *R.V. CEFAS Endeavour* for their assistance at sea, Caroline Limpenny (Centre for Environment, Fisheries and Aquaculture Science; CEFAS) for pre-cruise logistical support, and Jennifer Williams and Patrick Keenan at the Centre for Ecology and Hydrology (CEH) for assistance with the DOC analyses. SCP would like to thank the CEnd18/16 survey scientific party, Ben Hatton (Princ. Sci.) and Ian Holmes (2IC) for accommodating him during the 2016 Quarter 3 English International Beam Trawl Survey of the North Sea. Ferrybox data from the R.V. CEFAS *Endeavour* were provided courtesy of Tom Hull. Further details of the cruise are available on the CEFAS website (https://www.cefas.ac.uk/). DJL publishes with the permission of the Executive Director, British Geological Survey (NERC). This work contributes to Land Ocean Carbon Transfer (LOCATE; http://locate.ac.uk) a study supported by Natural Environment Research Council grant NE/N018087/1. All datasets are available via the British Oceanographic Data Centre (www.bodc.ac.uk) The views expressed are those of the authors and do not necessarily represent those of NERC or Defra.

References

Astoreca, R., Rousseau, V., Lancelot, C., 2009. Coloured dissolved organic matter (CDOM) in Southern North Sea waters: optical characterization and possible origin. Estuar. Coast. Shelf Sci. 85, 633–640.
Benner, R., Kaiser, K., 2011. Biological and photochemical transformations of amino acids and lignin phenols in riverine dissolved organic matter. Biogeochemistry 102, 209–222.
Bianchi, T.S., 2007. Biogeochemistry of Estuaries. Oxford University Press, Oxford (706 pages).
Bianchi, T.S., 2011. The role of terrestrially derived organic carbon in the coastal ocean: a changing paradigm and the priming effect. Proc. Natl. Acad. Sci. 108 (49), 19473–19481.
Bianchi, T.S., Rolff, C., Lambert, C.D., 1997. Sources and composition of particulate organic carbon in the Baltic Sea: the use of plant pigments and lignin-phenols as biomarkers. Mar. Ecol. Prog. Ser. 156, 25–31.
Bianchi, T.S., Osburn, C., Shields, M.R., Yvon-Lewis, S., Young, J., Guo, L., Zhou, Z., 2014. Deepwater horizon oil in Gulf of Mexico waters after 2 years: transformation into the dissolved organic matter pool. Environmental Science & Technology 48 (16), 9288–9297.
Blaas, M., Kerkhoven, D., de Swart, H.E., 2001. Large-scale circulation and flushing characteristics of the North Sea under various climate forcings. Clim. Res. 18, 47–54.
Bristow, L.A., Jickells, T.D., Weston, K., Marca-Bell, A., Parker, R., Andrews, J.E., 2013. Tracing estuarine organic matter sources into the southern North Sea using C and N isotopic signatures. Biogeochemistry 113, 9–22.
Bro, R., 1997. PARAFAC. Tutorial and applications. Chemom. Intel. Lab. Syst. 38, 149–171.
Burdige, D.J., 2005. The burial of terrestrial organic carbon in marine sediments: a reassessment. Global Biogeochemal Cycles https://doi.org/10.1029/2004GB002368.
Burdige, D.J., Skoog, A.A., Gardner, K., 2000. Dissolved and particulate carbohydrates in contrasting marine sediments. Geochim. Cosmochim. Acta 64, 1029–1041.
Butman, D.E., Wilson, H.F., Barnes, R.T., Xenopoulos, M.A., Raymond, P.A., 2015. Increased mobilization of aged carbon to rivers by human disturbance. Nat. Geosci. 8 (2), 112–116.
Cawley, K.M., Ding, Y., Fourqurean, J., Jaffe, R., 2012. Characterising the sources and fate of dissolved organic matter in Shark Bay, Australia: a preliminary study using optical properties and stable carbon isotopes. Marine and Fresehwater Research 63, 1098–1107.
Ciais, P., Sabine, C., Bala, G., Bopp, L., Brovkin, V., Canadell, J., Chhabra, A., DeFries, R., Galloway, J., Heimann, M., Jones, C., Le Quéré, C., Myneni, R.B., Piao, S., Thornton, P., 2013. Carbon and other biogeochemical cycles. In: Stocker, T.F., Qin, D., Plattner, G.-K., Tignor, M., Allen, S.K., Boschung, J., Nauels, A., Xia, Y., Bex, V., Midgley, P.M. (Eds.), Climate Change 2013: The Physical Science Basis. Contribution of Working Group I to the Fifth Assessment Report of the Intergovernmental Panel on Climate Change. Cambridge University Press, Cambridge, United Kingdom and New York, NY, USA.
Coble, P.G., 1996. Characterization of marine terrestrial DOM in seawater using excitation-emission matrix spectroscopy. Mar. Chem. 51, 325–346.
Coble, P.G., Spencer, R.G.M., Baker, A., Reynolds, D.M., 2014. Aquatic organic matter fluorescence. In: Coble, P.G., Lead, J., Baker, A., Reynolds, D.M., Spencer, R.G.M. (Eds.), Aquatic Organic Matter Fluorescence. Cambridge University Press, Cambridge, UK, pp. 75–122.
Core Team, R., 2016. R: A Language and Environment for Statistical Computing. Vienna, Austria, R Foundation for Statistical Computing https://www.R-project.org/.
Dai, M., Yin, Z., Meng, F., Liu, Q., Cai, W.-J., 2012. Spatial distribution of riverine DOC inputs to the ocean: an updated global synthesis. Curr. Opin. Environ. Sustain. 4, 170–178.
Dittmar, T., Stubbins, A., 2014. Dissolved Organic Matter in Aquatic Systems. In: Holland, H., Turekian, K. (Eds.), Treatise on Geochemistry, second edition 12, pp. 125–156.
Eatherall, A., Naden, P.S., Cooper, D.M., 1998. Simulating carbon flux to the estuary: the first step. Sci. Total Environ. 210/211, 519–533.
Evans, C.D., Page, S.E., Jones, T., Moore, S., Gauci, V., Laiho, R., Hruška, J., Allott, T.E.H., Billett, M.F., Tipping, E., Freeman, C., Garnett, M.H., 2014. Contrasting vulnerability of drained tropical and high-latitude peatlands to fluvial loss of stored carbon. Glob. Biogeochem. Cycles 28, 1215–1234.
Fichot, C.G., Benner, R., 2012. The spectral slope coefficient of chromophoric dissolved organic matter (S_{275_295}) as a tracer of terrigenous dissolved organic carbon in river-influenced ocean margins. Limnol. Oceanogr. 57 (5), 1453–1466.

Føyn, L., Rey, F., 1981. Nutrient distribution along the Norwegian Coastal Current. In: Saetre, R., Mork, M. (Eds.), The Norwegian Coastal Current. vol 2. University of Bergen, pp. 629–639.
Gonçalves-Araujo, R., Stedmon, C.A., Heim, B., Dubinenkov, I., Kraberg, A., Moiseev, D., Bracher, A., 2015. From fresh to marine waters: characterization and fate of dissolved organic matter in the Lena River Delta Region, Siberia. Front. Mar. Sci. 2:108. https://doi.org/10.3389/fmars.2015.00108.
Graeber, D., Gelbrecht, J., Pusch, M.T., Anlanger, C., von Schiller, D., 2012. Agriculture has changed the amount and composition of dissolved organic matter in Central European headwater streams. Sci. Total Environ. 438, 435–446.
Gustafsson, B.G., Andersson, H.C., 2001. Modeling the exchange of the Baltic sea from the meridional atmospheric pressure difference across the North Sea. J. Geophys. Res. 106, 19731–19744.
Gustafsson, E., Deutsch, B., Gustafsson, B.G., Humborg, C., Mörth, C.-M., 2014. Carbon cycling in the Baltic Sea - the fate of allocthonous organic carbon and its impact on air-sea CO_2 exchange. J. Mar. Syst. 129, 289–302.
Hansell, D.A., Carlson, C.A., Repeta, D.J., Schlitzer, R., 2009. Dissolved organic matter in the ocean: a controversy stimulates new insights. Oceanography 22 (4), 202–211.
Hedges, J.I., Keil, R., 1995. Sedimentary organic matter preservation: an assessment and speculative synthesis. Mar. Chem. 49, 81–115.
Hedges, J.I., Keil, R.G., Benner, R., 1997. What happens to terrestrial organic matter in the ocean? Org. Geochem. 27 (5/6), 195–212.
Helms, J.R., Stubbins, A., Ritchie, J.D., Minor, E.C., Kieber, D.J., Mopper, K., 2008. Absorption spectral slopes and slope ratios as indicators of molecular weight, source and photobleaching of chromophoric organic matter. Limnol. Oceanogr. 53 (3), 955–969.
Højerslev, N.K., 1981. Optical water mass classification in the Skagerrak and the eastern North Sea. In: Saetre, R., Mork, M. (Eds.), The Norwegian Coastal Current. vol 1. University of Bergen, pp. 331–339.
Huthnance, J.M., 1991. Physcial oceanography of the North Sea. Ocean and Shoreline Management. 16, pp. 199–231.
Huthnance, J.M., Holt, J.T., Wakelin, S.L., 2009. Deep ocean exchange with west-European shelf seas. Ocean Sci. 5, 621–634.
Hydes, D.J., Aoyama, M., Aminot, A., Bakker, K., Becker, S., Coverly, S., Daniel, A., Dickson, A. G., Grosso, O., Kerouel, R., van Ooijen, J., Sato, K., Tanhua, T., Woodward, E.M.S., Zhang, J.Z., 2010. Determination of dissolved nutrients (N, P, Si) in seawater with high precision and inter-comparability using gas-segmented continuous flow analysers. The GO-Ship Repeat Hydrography Manual: A Collection of Expert Reports and Guidelines. IOCCP Report No. 14, ICPO Publication Series No. 134 Version 1, 2010, pp. 1–87.
Jørgensen, L., Stedmon, C.A., Kragh, T., Markager, S., Middelboe, M., Søndergaard, M., 2011. Global trends in the fluorescence characteristics and distribution of marine dissolved organic matter. Mar. Chem. 126, 139–148.
Kalle, K., 1956. Chemisch-hydrographische Untersuchungen in der inneren Deutschen Bucht. Deutsche Hydrographische Zeitschrift 9 (2), 55–65.
Kothawala, D.N., Murphy, K.R., Stedmon, C.A., Weyhenmeyer, G.A., Tranvik, L.J., 2013. Inner filter correction of dissolved organic matter fluorescence. Limnol. Oceanogr. Methods 11, 616–630.
Kowalczuk, P., Stedmon, C.A., Markager, S., 2006. Modeling absorption by CDOM in the Baltic Sea from season, salinity and chlorophyll. Mar. Chem. 101, 1–11.
Kritzberg, E.S., Ekström, S.M., 2012. Increasing iron concentrations in surface waters – a factor behind brownification? Biogeosciences 9, 1465–1478.
Kulinski, K., Pempkowiak, J., 2011. The Carbon Budget of the Baltic Sea. Biogeosciences 8: 3219–3230. https://doi.org/10.5194/bg-3218-3219-2011.
Laane, R.W.P.M., Kramer, K.J.M., 1990. Natural fluorescence in the North Sea and its major estuaries. Neth. J. Sea Res. 26 (1), 1–9.
Lacroix, G., Ruddick, K., Ozer, J., Lancelot, C., 2004. Modelling the impact of the Scheldt and Rhine/Meuse plumes on the salinity distribution in Belgian waters (southern North Sea). J. Sea Res. 52, 149–163.
Lakowicz, J.R., 2006. Principles of Fluorescence Spectroscopy. 3rd edition. Springer (954 pp).
Le Quere, C., Andrew, R.M., Canadell, J.G., Sitch, S., Korsbakken, J.I., Peters, G.P., Manning, A. C., Boden, T.A., Tans, P.P., Houghton, R.A., Keeling, R.F., Alin, S., Andrews, O.D., Anthoni, P., Barbero, L., Bopp, L., Chevallier, F., Chini, L.P., Ciais, P., Currie, K., Delire, C., Doney, S. C., Friedlingstein, P., Gkritzalis, T., Harris, I., Hauck, J., Haverd, V., Hoppema, M., Goldewijk, K.K., Jain, A.K., Kato, E., Körtzinger, A., Landschützer, P., Lefèvre, N., A., L., Lienert, S., Lombardozzi, D., Melton, J.R., Metzl, N., Millero, F., Monteiro, P.M.S., Munro, D.R., Nabel, J.E.M.S., Nakaoka, S.-I., O'Brien, K., Olsen, A., Omar, A.M., Ono, T., Pierrot, D., Poulter, B., Rödenbeck, C., Salisbury, J., Schuster, U., Schwinger, J., Séférian, R., Skjelvan, I., Stocker, B.D., Sutton, A.J., Takahashi, T., Tian, H., Tilbrook, B., van der Laan-Luijkx, I.T., van der Werf, G.R., Viovy, N., Walker, A.P., Wiltshire, A.J., Zaehle, S., 2016. Global carbon budget 2016. Earth System Science Data 8, 605–649.
Lee, A.J., 1980. North Sea: physical oceanography. In: Banner, F.T., Collins, M.B., Massie, K. S. (Eds.), The North-West European Shelf Seas: The Sea Bed and the Sea in Motion II. Physical and Chemical Oceanography, and Physical Resources, pp. 467–493.
Lübben, A., Dellwig, O., Koch, S., Beck, M., Badewien, T.H., Fischer, S., Reuter, R., 2009. Distributions and characteristics of dissolved organic matter in temperate coastal waters (Southern North Sea). Ocean Dyn. 59, 263–275.
Maasicotte, P., Asmala, E., Stedmon, C., Markager, S., 2017. Global distribution of dissolved organic matter along the aquatic continuum: across rivers, lakes and oceans. Sci. Total Environ. 609, 180–191.
Massicotte, P., Markager, S., 2016. Using a Gaussian decomposition approach to model absorption spectra of chromophotic dissolved organic matter. Mar. Chem. 180, 24–32.
Mcknight, D.M., Boyer, E.W., Westerhoff, P.K., Doran, P.T., Kulbe, T., Andersen, D.T., 2001. Spectrofluorometric characterization of dissolved organic matter for indication of precursor organic material and aromaticity. Limnol. Oceanogr. 46, 38–48.
Meler, J., Kowalczuk, P., Ostrowska, M., Ficek, C., Zablocka, M., Zdun, A., 2016. Parameterization of the light absorption properties of chromophoric dissolved organic matter in the Baltic Sea and Pomeranian lakes. Ocean Science 12:1013–1032. https://doi.org/10.5195/os-1012-1013-2016.
Monteith, D.T., Stoddard, J.L., Evans, C.D., de Wi, H., Forsius, M., Høgåsen, T., Wilander, A., Skjelkvåle, B.L., Jeffries, D.S., Vuorenmaa, J., Keller, B., Kopácek, J., Vesely, J., 2007. Dissolved organic carbon trends resulting from changes in atmospheric deposition chemistry. Nature 450, 537–540.
Moore, W.S., 2010. The effect of submarine groundwater discharge on the ocean. Annual Reviews in Marine Science 2, 59–88.
Moore, W.S., Beck, M., Riedel, T., Rutgers van der Loeff, M., Dellwig, O., Shaw, T.J., Schnetger, B., Brumsack, H.-J., 2011. Radium-based pore water fluxes of silica, alkalinity, manganese, DOC, and uranium: a decade of studies in the German Wadden Sea. Geochim. Cosmochim. Acta 75, 6535–6555.
Moran, M.A., Sheldon, W.M., Zepp, R.G., 2000. Carbon loss and optical property changes during long-term photochemical and biological degradation of estuarine dissolved organic matter. Limnol. Oceanogr. 45, 1254–1264.
Murphy, K.R., Stedmon, C.A., Waite, T.D., Ruiz, G.M., 2008. Distinguishing between terrestrial and autochthonous organic matter sources in marine environments using fluorescence spectroscopy. Mar. Chem. 108, 40–58.
Murphy, K.R., Butler, K.D., Spencer, R.G.M., Stedmon, C.A., Boehme, J.R., Aiken, G.R., 2010. Measurement of dissolved organic matter fluorescence in aquatic environments: an interlaboratory comparison. Environmental Science & Technology 44, 9405–9412.
Murphy, K.R., Hambly, A., Singh, S., Henderson, R.K., Baker, A., Stuetz, R., Khan, S.J., 2011. Organic matter fluorescence in municipal water recycling schemes: toward a unified PARAFAC model. Environmental Science & Technology 45, 2909–2916.
Murphy, K.R., Stedmon, C.A., Graeber, D., Bro, R., 2013. Fluorescence spectroscopy and multi-way techniques. PARAFAC. Anal. Methods 5, 6557–6566.
Murphy, K.R., Stedmon, C.A., Wenig, P., Bro, R., 2014a. OpenFluor - an online spectral library of auto-fluorescence by organic compounds in the environment. Anal. Methods 6, 658–661.
Murphy, K.R., Bro, R., Stedmon, C.A., 2014b. Chemometric analysis of organic matter fluorescence. In: Coble, P.G., Lead, J., Baker, A., Reynolds, D.M., Spencer, R.G.M. (Eds.), Aquatic Organic Matter Fluorescence. Cambridge University Press, Cambridge, UK, pp. 339–375.
Neal, C., Jarvie, H.P., Williams, R.J., Pinder, L.C.V., Collett, G.D., Neal, M., Bhardwaj, L., 2000. The water quality of the Great Ouse. Sci. Total Environ. 251 (252), 423–440.
Opsahl, S., Benner, R., 1997. Distribution and cycling of terrigenous dissolved organic matter in the ocean. Nature 386, 480–482.
Opsahl, S., Benner, R., 1998. Photochemical reactivity of dissolved lignin in river and ocean waters. Limnol. Oceanogr. 43 (6), 1297–1304.
Osburn, C.L., Stedmon, C.A., 2011. Linking the chemical and optical properties of dissolved organic matter in the Baltic–North Sea transition zone to differentiate three allochthonous inputs. Mar. Chem. 126, 281–294.
Osburn, C.L., Handsel, L.T., Mikan, M.P., Paerl, H.W., Montgomery, M.T., 2012. Fluorescence tracking of dissolved and particulate organic matter quality in a river-dominated estuary. Environmental Science & Technology 46, 8628–8636.
OSPAR Commission, 2003. Nutrients in the Convention area: inputs of nutrients into the convention area. Implementation of PARCOM Recommendations 88/2 and 89/4, OSPAR (55 pages).
OSPAR Commission, 2008. Towards the 50% reduction target for nutrients. Assessment of Implementation of PARCOM Recommendations 88/2 and 89/4. OSPAR (115 pages).
OSPAR Commission, 2016. Riverine Inputs and Direct Discharges to Convention waters: OSPAR Contracting Parties' RID 2014 Data Report. OSPAR (83 pages).
Otto, L., Zimmerman, J.T.F., Furness, G.K., Mork, M., Saetre, R., Becker, G., 1990. Review of the physical oceanography of the North Sea. Neth. J. Sea Res. 26 (2–4), 161–238.
Prandle, D., 1984. A modelling study of the mixing of ^{137}Cs in the seas of the European Continental Shelf. Phil. Trans. R. Soc. A 310, 407–436.
Radach, G., 1998. Quantification of long-term changes in the German Bight using an ecological development index. ICES J. Mar. Sci. 55, 587–599.
Radach, G., Gekeler, J., 1996. Annual cycles of horizontal distributions of temperature and salinity, and of concentrations of nutrients, suspended particulate matter and chlorophyll on the northwest European shelf. Deutsche Hydrographische Zeitschrift 48 (3/4), 261–297.
Radach, G., Patsch, J., 1997. Climatological annual cycles of nutrients and chlorophyll in the North Sea. J. Sea Res. 38, 231–248.
Räike, A., Kortelainen, P., Mattsson, T., Thomas, D.N., 2012. 36 year trends in dissolved organic carbon export from Finnish rivers to the Baltic Sea. Sci. Total Environ. 435-436, 188–201.
Raike, A., Kortelainen, P., Mattsson, T., Thomas, D.N., 2016. Long-term trends (1975-2014) in the concentrations and export of carbon from Finnish rivers to the Baltic Sea: organic and inorganic components compared. Aquat. Sci. 78:505–523. https://doi.org/10.1007/s00027-00015-00451-00022.
Seidel, M., Manecki, M., Herlemann, D.P.R., Deutsch, B., Schulz-Bull, D., Jürgens, K., Dittmar, T., 2017. Composition and transformation of dissolved organic matter in the Baltic Sea. Front. Earth Sci. 5, 31. https://doi.org/10.3389/feart.2017.00031.
Sholkovitz, E.R., Boyle, E.A., Price, N.B., 1978. The removal of dissolved humic acids and iron during estuarine mixing. Earth Planet. Sci. Lett. 40, 130–136.
Shutova, Y., Baker, A., Bridgeman, J., Henderson, R.K., 2014. Spectroscopic characterisation of dissolved organic matter changes in drinking water treatment: from PARAFAC analysis to online monitoring wavelengths. Water Res. 54, 159–169.
Slomp, C.P., Van Cappellen, P., 2004. Nutrient inputs to the coastal ocean through submarine groundwater discharge: controls and potential impact. J. Hydrol. 295 (1–4), 64–86.
Søndergaard, M., Stedmon, C.A., Borch, N.H., 2003. Fate of terrigenous dissolved organic matter (DOM) in estuaries: aggregation and bioavailability. Ophelia 57 (3), 161–176.
Stedmon, C.A., Bro, R., 2008. Characterising dissolved organic matter fluorescence with parallel factor analysis: a tutorial. Limnol. Oceanogr. Methods 6, 572–579.

Stedmon, C.A., Markager, S., 2001. The optics of chromophoric dissolved organic matter (CDOM) in the Greenland Sea: an algorithm for differentiation between marine and terrestrially derived organic matter. Limnol. Oceanogr. 46 (8), 2087–2093.
Stedmon, C.A., Markager, S., 2003. Behaviour of the optical properties of coloured dissolved organic matter under conservative mixing. Estuar. Coast. Shelf Sci. 57, 973–979.
Stedmon, C.A., Markager, S., 2005. Resolving the variability in dissolved organic matter fluorescence in a temperate estuary and its catchment using PARAFAC analysis. Limnol. Oceanogr. 50 (2), 686–697.
Stedmon, C.A., Nelson, N.B., Hansell, D.A., Carlson, C.A., 2015. The optical properties of DOM in the ocean. Biogeochemistry of Marine Dissolved Organic Matter (2nd Edition). Academic Press, Amsterdam, pp. 481–508.
Stedmon, C.A., Markager, S., Bro, R., 2003. Tracing dissolved organic matter in aquatic environments using a new approach to fluorescence spectroscopy. Mar. Chem. 82, 239–254.
Stedmon, C.A., Osburn, C.L., Kragh, T., 2010. Tracing water mass mixing in the Baltic–North Sea transition zone using the optical properties of coloured dissolved organic matter. Estuar. Coast. Shelf Sci. 87, 156–162.
Stuart, M.E., Lapworth, D.J., 2016. Macronutrient status of UK groundwater: nitrogen, phosphorus and organic carbon. Sci. Total Environ. 572, 1543–1560.
Swarzenski, P.W., Simonds, F.W., Paulson, A.J., Kruse, S., Reich, C., 2007. Geochemical and geophysical examination of submarine groundwater discharge and associated nutrient loading estimates into Lynch Cove, Hood Canal, WA. Environmental Science & Technology 41 (20), 7022–7029.
Thomas, H., Pempowiak, J., Wulff, F., Nagel, K., 2010. The Baltic sea. In: Liu, K.-K., Atkinson, L., Quinones, R.A., Talaue-McManus, L. (Eds.), Carbon and Nutrient Fluxes in Continental Margins. Springer-Verlag, Berlin, pp. 334–346.
Torres-Valdes, S., Tsubouchi, T., Davey, E., Yashayaev, I., Bacon, S., 2016. Relevance of dissolved organic nutrients for the Arctic Ocean nutrient budget. Geophysical Research Letters 43:6418–6426. https://doi.org/10.6102/2016GL069245.
Tranvik, L.J., Downing, J.A., Cotner, J.B., Loiselle, S.A., Striegl, R.G., Ballatore, T.J., Dillon, P., Finlay, K., Fortino, K., Knoll, L.B., Kortelainen, P.L., 2009. Lakes and reservoirs as regulators of carbon cycling and climate. Limnol. Oceanogr. 54 (6part2), 2298–2314.
Turrell, W.R., Henderson, E.W., Slesser, G., 1990. Residual transport within the Fair Isle Current observed during the Autumn Circulation Experiment (ACE). Cont. Shelf Res. 10 (6), 521–543.
Turrell, W.R., Henderson, E.W., Slesser, G., Payne, R., Adams, R.D., 1992. Seasonal changes in the circulation of the northern North Sea. Cont. Shelf Res. 12 (2–3), 257–286.
UNESCO, 2010. The International Thermodynamic Equation of Seawater - 2010: Calculation and Use of Thermodynamic Properties. International Oceanographic Commission, p. 171.
Vodacek, A., Blough, N.V., DeGranpre, M.D., Peltzer, E.T., Nelson, R.K., 1997. Seasonal variation of CDOM and DOC in the Middle Atlantic Bight: terrestrial inputs and photooxidation. Limnol. Oceanogr. 42 (4), 674–686.
Voss, M., Baker, A., Bange, H.W., Conley, D., Cornell, S., Deutsch, B., Engel, A., Ganeshram, R., Garnier, J., Heiskanen, A.-S., Jickells, T., Lancelot, C., McQuatters-Gollop, A., Middelburg, J., Schiedek, D., Slomp, C.P., Conley, D.P., 2011. Nitrogen processes in coastal and marine ecosystems. In: Sutton, M.A., Howard, C.M., Erisman, J.W., Billen, G., Bleeker, A., Grennfelt, P., van Grinsven, H., G., B. (Eds.), The European Nitrogen Assessment. Cambridge, Cambridge University Press, pp. 147–176.
Walker, S.A., Amon, R.M.W., Stedmon, C., Duan, S., Louchouran, P., 2009. The use of PARAFAC modeling to trace terrestrial dissolved organic matter and fingerprint water masses in coastal Canadian Arctic surface waters. Journal of Geophysical Research 114, G00F06. https://doi.org/10.1029/2009JG00990.
Ward, N.D., Bianchi, T.S., Medeiros, P.M., Seidel, M., Richey, J.E., Keil, R.G., Sawakuchi, H.O., 2017. Where carbon goes when water flows: carbon cycling across the aquatic continuum. Front. Mar. Sci. 4, 7. https://doi.org/10.3389/fmars.2017.00007.
Warnock, R.E., Gieskes, W.W.C., van Laar, S., 1999. Regional and seasonal differences in light absorption by yellow substance in the Southern Bight of the North Sea. J. Sea Res. 42, 169–178.
Weishaar, J.L., Aiken, G.R., Bergamaschi, B.A., Fram, M.S., Fujii, R., Mopper, K., 2003. Evaluation of specific ultraviolet absorbance as an indicator of the chemical composition and reactivity of dissolved organic carbon. Environmental Science & Technology 37, 4702–4708.
Whetten, R., Sederoff, R., 1995. Lignin biosynthesis. Plant Cell 7, 1001–1013.
Woodward, E.M.S., Owens, N.J.P., 1990. Nutrient depletion studies in offshore North Sea areas. The. Neth. J. Sea Res. 25, 57–63.
Woodward, E.M.S., Rees, A.P., 2001. Nutrient distributions in an anticyclonic eddy in the North East Atlantic Ocean, with reference to nanomolar ammonium concentrations. Deep-Sea Res. 48:775–794. https://doi.org/10.1016/S0967-0645(00)00097-7.
Worrall, F., Burt, T.P., 2007. Flux of dissolved organic carbon from U.K. rivers. Global Biogeochem. Cycles 21, GB1013. https://doi.org/10.1029/2006GB002709.
Worrall, F., Davies, H., Bhogal, A., Lilly, A., Evans, M., Turner, K., Burt, T., Barraclough, D., Smith, P., Merrington, G., 2012. The flux of DOC from the UK – predicting the role of soils, land use and net watershed losses. J. Hydrol. 448-449, 149–160.
Yamashita, Y., Tanoue, E., 2003. Chemical characterization of protein-like fluorophores in DOM in relation to aromatic amino acids. Mar. Chem. 82, 255–271.
Yamashita, Y., Jaffe, R., Maie, N., Tanoue, E., 2008. Assessing the dynamics of dissolved organic matter (DOM) in coastal environments by excitation emission matrix fluorescence and parallel factor analysis (EEM-PARAFAC). Limnol. Oceanogr. 53 (5), 1900–1908.
Yamashita, Y., Kloeppel, B.D., Knoepp, J., Zausen, G.L., Jaffe, R., 2011a. Effects of watershed history on dissolved organic matter characteristics in headwater streams. Ecosystems 14, 1110–1122.
Yamashita, Y., Panton, A., Mahaffey, C., Jaffe, R., 2011b. Assessing the spatial and temporal variability of dissolved organic matter in Liverpool Bay using excitation-emission matrix fluorescence and parallel factor analysis. Ocean Dyn. 61, 569–579.
Yamashita, Y., Boyer, J.N., Jaffe, R., 2013. Evaluating the distribution of terrestrial dissolved organic matter in a complex coastal ecosystem using fluorescence spectroscopy. Cont. Shelf Res. 66, 136–144.